International Journal of Pharmaceutical Research and Applications
Volume 7, Issue 3 May-June 2022, pp: 1529-1558 www.ijprajournal.com ISSN: 2456-4494

Formulation and Characterization of Floating Microspheres of Rabeprazole Sodium

Parvin Tarannun, Shukla Amit Kumar, Mishra Dr. J. N.

1. Parvin Tarannun (PG Scholar) Kailash Institute of Pharmacy and Management GIDA, Gorakhpur Uttar Pradesh, India

*2. *Shukla Amit Kumar (Associate Professor) Kailash Institute of Pharmacy and Management GIDA, Gorakhpur Uttar Pradesh, India*

3. Mishra Dr. J. N. (Director) Kailash Institute of Pharmacy and Management GIDA, Gorakhpur Uttar Pradesh, India

Submitted: 01-06-2022 Revised: 14-06-2022 Accepted: 16-06-2022

ABSTRACT

Rabeprazole sodium is an antiulcer drug in the class of proton pump inhibitors. It is a prodrug in the acid environment of the parietal cells it turns into active sulphenamide form. Rabeprazole inhibits the H^+/K^+ ATPase enzyme of the coating gastric cells and dose- dependent suppresses basal and stimulated gastric acid secretion. The main objective of the present research is exploring the floating microspheres of Rabeprazole sodium using different polymers. Nine formulations of floating microspheres of Rabeprazole sodium have been prepared by using different concentrations of polymers. Floating microspheres of Rabeprazole sodiumwere prepared by "Emulsion Solvent Evaporation Technique"**.**

The FT-IR spectrum and UV-spectrum (λ_{max}= 283.7 nm) confirm the purity of Rabeprazole sodium. Result of compatibility study showed that there were no interaction among the polymers and Rabeprazole sodium. The mean particle size ranged from 85.32 ±3.213 µm to 167.43±4.532 µm. SEM revealed a hollow spherical structure of microspheres with a smooth surface morphology and the internal surface was porous due to the evaporation of solvent entrapped within the shell of microspheres.

The percentage buoyancy of all the formulations was found to be in the range of 62.21±1.337% - 82.70±0.676%. As the concentration of polymers increases, buoyancy also increases. The percentage entrapment efficiency for the formulations (RZS1, RZS2 and RZS3) was found to be 69.89±1.832% to 77.68±1.173%. The percentage entrapment efficiency for the formulations (RZS4, RZS5 and RZS6) was found to be 66.93±0.821% to 70.69±1.363%. The percentage entrapment efficiency for the formulations (RZS7, RZS8 and RZS9) was found to be 66.93±1.641% to 73.65 ± 0.721%.

The results of the in vitro dissolution studies shows controlled and predictable manner as the polymer concentration increases the drug release from the floating microsphere decreases.

Keyword: Rabeprazole sodium, floating microspheres, solvent evaporation, flow properties, drug release kinetics.

I. INTRODUCTION

The methods, formulations, technologies, and systems for delivering a pharmaceutical chemical in the body as needed to safely achieve the desired therapeutic effects are referred to as Novel Drug Delivery Systems (NDDS). It could involve scientific site-targeting within the body or aiding systemic pharmacokinetics; in any event, it's usually about the quantity and duration of drug presence." Novel drug delivery is often achieved through the chemical composition of a drug, but can also be achieved through medical devices or drug combination solutions. The concept of drug delivery is closely related to the type of dosage and route of administration. NDDS is a sophisticated drug delivery system that improves drug efficacy, regulates drug release for a longer-lasting therapeutic effect, increases safety, and ultimately targets a drug to a specific tissue. NDDS is a drug delivery method that differs from other drug delivery systems. NDDS is a combination of cutting-edge technology and novel dosage forms that outperform traditional dosage forms [4, 5]. The oral route is the most common and preferred method of drug delivery, however despite excellent in vitro release patterns, drug absorption is inadequate and extremely varied among individuals[7]. Apart from the numerous benefits of oral drug delivery, it also faces problems such as

International Journal of Pharmaceutical Research and Applications
Volume 7, Issue 3 May-June 2022, pp: 1529-1558 www.ijprajournal.com ISSN: 2456-4494

limited bioavailability due to gastrointestinal heterogeneity, commensal flora pH, dose form gastric retention duration, surface area, and enzymatic activity8. Traditional drug delivery technologies are unable to address the aforementioned issues. As a result, Gastroretentive Drug Delivery Systems (GRDDS), a new drug delivery method, enters the scene. Microspheres are broadly disseminated along the gastrointestinal tract due to their small particle size, which improves drug absorption and reduces side effects caused by localized buildup of irritating drug against the gastrointestinal mucosa. The medication is released slowly and at the desired rate in a microsphere, resulting in less volatility in plasma drug concentration, enhanced bioavailability, increased drug half-life, reduced drug wastage, and improved patient compliance by minimizing recurrent dose[40]. Floating Microspheres (Hollow Microspheres) are non-effervescent methods of drug delivery that are gastroretentive. Hollow microspheres in the narrower sense are spherical empty particles without a core, free-flowing powder made of proteins or synthetic polymers in the size range of 1-1000 microns. The air trapped by the expanded polymer reduces the density of the microspheres and gives them buoyancy. However, to achieve adequate buoyancy, a minimum stomach content is required [46, 47].

II. MATERIAL AND METHOD

Ulcers can be addressed with the help of the proton pump inhibitor rabeprazole sodium. Parietal cells are acidic and sulphenamide can be converted to its active form in the presence of this environment. Rabeprazole inhibits the H+/K+ ATPase enzyme in the coated gastric cells, resulting in a dose-dependent reduction in both baseline and provoked gastric acid output.

Fig. 1: Chemical structure of Rabeprazole sodium

- **IUPAC NAME**: 2-({[4-(3-Methoxypropoxy)-3-methyl-2-pyridyl] methyl} sulfinyl) -1H-benzimidazole sodium
- **Empirical formula**: $C_{18}H_{20}N_3O_3S.Na$
- **Molecular weight**: 381.43
- **Melting point**: 140-141^{0}C
- **Description**: A white to yellowish crystalline powder.
- **Category**: Proton Pump Inhibitor
- **Solubility**: It is very soluble in water and methanol, freely soluble in ethanol, chloroform and ethyl acetate and insoluble in ether and n-hexane.
- **Standard:** Rabeprazole sodium contains not less than 98.5% and not more than 101.5% of $C_{18}H_{20}N_3O_3S.Na$ calculated with reference to the dried substance.
- **Half life:** 1-2 hours (in plasma)
- **Absorption:** Absolute bioavailability is approximately 52%
- **Volume of distribution:** 160 liter
- **Protein binding:** 96.3% (bound to human plasma proteins)

Method

Preliminary studies and preformulation

Rabeprazole sodium procurement and identification

MARC India Limited, Baddi, Solan, Himachal Pradesh, provided a complimentary sample of Rabeprazole sodium (India). Rabeprazole sodium was a white to light yellowish-white crystalline powder in its purest form. Silicon oil digital melting point device was used to determine the melting point of Rabeprazole sodium. The melting point was discovered to be between 140 and 142°C.

Rabeprazole sodium solubility determination

In distilled water, methanol, ethanol, chloroform, ethyl acetate, ether, and hexane, the solubility of Rabeprazole sodium was determined.

FT-IR spectroscopy was used to characterise Rabeprazole sodium.

FT-IR (Fourier Transform Infrared Spectroscopy) spectroscopy was used to record the spectra of pure Rabeprazole sodium (Shimadzu-8400 S, Japan). KBr pellets were made by mixing KBr with pure medication and triturate in a mortar

International Journal of Pharmaceutical Research and Applications
Volume 7, Issue 3 May-June 2022, pp: 1529-1558 www.ijprajournal.com ISSN: 2456-4494

for FT-IR spectra. Pellets were formed by crushing fine powder in a pressing machine. In the FTIR, the prepared pellet was scanned across a frequency range of 4000 to 400 cm-1.

Rabeprazole sodium maximum concentration

A ready-made solution The volume was made to 100 ml with 0.1N HCl (1000 g/ml) after 100 mg of Rabeprazole sodium was accurately weighed.

A 10 g/ ml solution of Rabeprazole sodium was produced from stock solution in 0.1N hydrochloric acid, and max was determined using a UV-VIS double beam spectrophotometer (Shimadzu-1800, Japan). Between 200 and 400 nm, the solution was scanned.

The standard Rabeprazole sodium calibration curve

Rabeprazole sodium solutions of 10, 20, 30, 40, and 50 g/ml were produced in 0.1N hydrochloric acid from the stock solution. These solutions' absorbance was measured at 283.7 nm, and a concentration vs absorbance graph was generated.

Fourier Transform Infrared Spectroscopy investigation of drug-excipient compatibility

To ensure compatibility, rabeprazole sodium was put through its paces in the manufacturing of floating microspheres. To conduct a compatibility study, rabeprazole sodium was mixed 1:1 with a variety of polymers. Glass vials were used to store the liquid, which were then taped shut with Teflon tape. Temperatures were maintained at 252oC and 3720oC for a month, with two vials of each mixture. samples were obtained at regular intervals from each vial (i.e. 0th day, 10th days, 15th days, 20st days and 30th days). Rabeprazole sodium content was assessed by utilising a standard calibration curve for Rabeprazole sodium in each sample that was withdrawn. Each sample was examined for any physical alterations.

Using Fourier Transform Infrared Spectroscopy, the compatibility of Rabeprazole sodium with various polymers was investigated. FT-IR spectroscopy was used to record the IR spectra of pure Rabeprazole sodium and polymers (ethyl cellulose, hydroxypropyl methylcellulose K15M, eudragit S100) using the KBr pellet technique (Shimadzu-8400 S, Japan).

Rabeprazole sodium floating microsphere formulation methods

Using varying polymer concentrations, nine formulations of Rabeprazole sodium floating microspheres were created (Table 5.1). The "Emulsion Solvent Evaporation Technique" was used to make floating microspheres of Rabeprazole sodium.

Ethyl cellulose-Eudragit floating microspheres

The polymer ratios of ethyl cellulose to eudragit were 1:1, 1:2, and 1:3. Using a magnetic stirrer spinning at 100 revolutions per minute, we dispersed 200 mg of medicine (rabeprazole sodium) and a polymer combination in 40 ml of dichloromethane/ethanol (1:1) for 15 minutes. Polyvinyl alcohol solution containing Tween 80 was heated to 405°C, and the drug-polymer mixture was gently added to the 150 ml solution (as an emulsifying agent). For two hours at 500 rpm, a three-blade propeller stirred the mixture. Stirring was stopped as soon as the dichloromethane odour disappeared. The floating microspheres were collected using a simple decantation method. It was decided to dump all of the microsphere and polymer remnants that couldn't float. Before being stored in a desiccator filled with calcium chloride, the microspheres needed to be cleaned with excess n-hexane, petroleum ether, and dried at room temperature. To distinguish between the three different formulations, the letters RZS1–RZS3 were used.

HPMC K15M-Eudragit floating microspheres

All three of the polymer ratios used were HPMC K15M-Eudragit. There were no side effects seen after 15 minutes of stirring with a magnetic stirrer set to 100 revolutions per minute while dissolving 200 mg of the drug (rabeprazole sodium) and polymer combination in dichloromethane and ethanol (1:1). Drug and polymer combination was gradually put into 150 ml of 0.75 percent polyvinyl alcohol solution with Tween 80 at 405°C (as an emulsifying agent). For two hours at 500 rpm, a three-bladed propeller stirred the mixture. Until the dichloromethane odour disappeared, the stirring was halted The floating microspheres were collected by simple decantation. The microspheres and polymer waste were gathered and thrown to the bottom of the container. As soon as the microspheres had been collected and washed, they were dried at room temperature and stored in a desiccator containing calcium chloride as the desiccant. The formulas RZS4, RZS5, and RZS6 were referred to as RZS4 through RZS6.

Floating microspheres made of ethyl cellulose, HPMC K15M, and Eudragit

All three polymer ratios (Ethyl cellulose, HPMC K15M, and Eudragit) were used in the formulation. There were no side effects seen after

International Journal of Pharmaceutical Research and Applications
Volume 7, Issue 3 May-June 2022, pp: 1529-1558 www.ijprajournal.com ISSN: 2456-4494

15 minutes of stirring with a magnetic stirrer set to 100 revolutions per minute while dissolving 200 mg of the drug (rabeprazole sodium) and polymer combination in dichloromethane and ethanol (1:1). Drug and polymer combination was gradually put into 150 ml of 0.75 percent polyvinyl alcohol solution with Tween 80 at 405°C (as an emulsifying agent). For two hours at 500 rpm, a three-bladed propeller stirred the mixture. Until the dichloromethane odour disappeared, the stirring was halted The floating microspheres were collected by simple decantation. The microspheres and polymer waste were gathered and thrown to the bottom of the container. As soon as the microspheres had been collected and washed, they were dried at room temperature and stored in a desiccator containing calcium chloride as the desiccant. The formulas RZS7, RZS8, and RZS9 were referred to as RZS7, RZS8, and RZS9.

Table 1: Composition of floating microspheres of Rabeprazole sodium

Formulations	Drug : Polymer				Ethanol: Dichloromethane (1:1) ml	Conc. of PVA (0.75 w/v) ml	Tween 80 (%)
	RZS (mg)	Ethyl Cellulose (mg)	HPMC K15M (mg)	Eudragit S100 (mg)			
RZS1	200	200	---	200	40	150	0.5
RZS2	200	200	---	400	40	150	0.5
RZS3	200	200	---	600	40	150	0.5
RZS4	200	---	200	200	40	150	0.5
RZS5	200	---	200	400	40	150	0.5
RZS6	200	---	200	600	40	150	0.5
RZS7	200	200	200	200	40	150	0.5
RZS8	200	200	200	400	40	150	0.5
RZS9	200	200	200	600	40	150	0.5

Rabeprazole sodium floating microspheres evaluation

- Kinetics of zero-order release
- Kinetics of first order release
- Higuchi's release kinetics model

Yield of floating microspheres as a percentage

Each formulation's manufactured floating microspheres were thoroughly dried and weighed. Each formulation's % yield of floating microspheres was estimated using the following formula:

$$\text{Percentage yield} = \frac{\text{Practical yield}}{\text{Theoretical yield}}$$

Where,

Practical yield = Final weight of floatingmicrospheres

Theoretical yield = Initial weight of the drug and polymer

Bulk density determination

The USP method was used to calculate the bulk and tapped densities. When calculating bulk density, weight divided by volume equals bulk density. Floating microspheres in a 100 ml measuring cylinder were added, and the surface was levelled without the use of force in order to arrive at the calculation. The following formula was used to calculate bulk density:

$$\text{Bulk density} = \frac{\text{Weight of floating microsphere}}{\text{Volume of floating microsphere}}$$

A 100 ml measuring cylinder was filled with floating microspheres that had been pre-weighed. In order to attach the measuring cylinder, a bulk density test instrument was utilised. After 100 taps, the microsphere's volume was measured. The following calculation was used to calculate tapped density:

$$\text{Tapped density} = \frac{\text{Weight offloating microsphere}}{\text{Tapped volume of floating microsphere}}$$

International Journal of Pharmaceutical Research and Applications
Volume 7, Issue 3 May-June 2022, pp: 1529-1558 www.ijprajournal.com ISSN: 2456-4494

Reposing angle

An technique based on a fixed funnel was employed to calculate the floating microspheres' angle of repose (). Conveyor-mounted tripod stand was used to collect the floating microspheres. Microspheres were permitted to float freely in the funnel. The microspheres' height and radius were measured, and the angle of repose was computed using the following formula:

$$\tan\theta = \frac{\text{Hight of the heap of floating microsphere}}{\text{Radius of heap of floating microsphere}}$$

Carr's compressibility index

The compressibility index of the powder blend was determined by Carr's compressibility index with the help of following equation:

$$\text{Carr's compressibility index (\%)} = \frac{\text{Tapped density} - \text{Bulk density}}{\text{Tapped density}} \text{ x } 100$$

The Hausner Ratio

The flowing property of a powder or granular material was explained by Hausner's ratio. The Hausner's ratio is the ratio of tapped density to bulk density of a powder or granular material, and it is computed using the following formula:

$$\text{Hausner's ratio} = \frac{\text{Tapped density}}{\text{Bulked density}}$$

Analysis of particle size and particle size distributions

Particle size distributions analysis is the process of calculating the average particle size (diameter) of floating microspheres. An optical microscope was used to measure the microspheres' average diameters in the water. The average size of the floating microspheres was determined using a pre-calibrated ocular micrometre and a stage micrometre slide placed on a compound microscope. Each formulation's diameters were measured with 100 floating microspheres at random, and the average was calculated.

Surface morphology research (SEM analysis)

The surface morphology of the floating microspheres was studied using scanning electron microscopy (SEM). The platinum-coated aluminium stubs were scanned in the scanning electron microscopy chamber (JSM- 6660D, Tokyo, Japan) and microphotographs were obtained.

Percentage buoyancy in vitro

50 mg of floating microspheres were dispersed in 200 ml of pH 1.2 simulated stomach juice containing 0.02 percent w/v Tween 80. For 8 hours, a magnetic stirrer was employed to agitate the suspension at 100 rpm. Filtration was used to separate the microspheres that sank to the bottom of the medium from those that sank to the surface and were pipetted out. In a desiccator, both floating and sink microspheres were properly dried. The floating microspheres' % buoyancy was determined using the formula:

$$\text{Buoyancy (\%)} = \frac{\text{Weight of floating micorspheres}}{\text{Weight of floating micorspheres} + \text{Weight of settled microshpe}}$$

Determination of drug entrapment percentage

Floating microspheres with 10 mg of medication were used to calculate the entrapment percentage. After weighing the floating microspheres in a mortar, 100 ml 0.1N HCl was used to extract the material. After the drug was removed, the solution was filtered through a Whatman No. 41 filter paper. Following proper dilution, spectrophotometric analysis of an aliquot was performed. At 283.7 nm, the absorbance was measured against a blank of 0.1N HCl. The following equation was used to calculate drug entrapment efficiency.

$$\text{Percentage of drug entrapment} = \frac{\text{Actual drug content}}{\text{Theoretical drug content}} \text{ x } 100$$

Study of drug release in vitro

In vitro drug release parameters of each floating microsphere formulation were determined using a USP class I dissolving test apparatus. Rotational speed was set at 100 RPM and 37 2°C in the dissolution test apparatus' basket. The dissolution media was 900ml of 0.01 N HCl. In the dissolution medium, 25 mg of floating microspheres (Rabeprazole sodium) were weighed out and dispersed evenly. Filtered with Whatman filter paper, 10 mL of sample was collected at regular intervals. The volume was replaced with the same amount of new dissolving medium each time in order to preserve the sink state. Diluting the dissolution media samples with 0.1N HCI and conducting spectrophotometric analyses at 283.7 nm against blanks, the concentration of drug in the dissolution medium was determined.

Kinetic investigations of drug release

In vitro dissolution data were fitted in Zero order rate kinetics, First order rate kinetics,

International Journal of Pharmaceutical Research and Applications
Volume 7, Issue 3 May-June 2022, pp: 1529-1558 www.ijprajournal.com ISSN: 2456-4494

and Higuchi's model to investigate the process of drug release from floating microspheres.

III. RESULTS AND DISCUSSION

Preformulation and Preliminary studies

Identification and characterization of Rabeprazole sodium

The pure sample of Rabeprazole sodium was white to off-white solid powder. The melting point of Rabeprazole sodium was determined by silicon oil digital melting point apparatus and the melting point was found to be 140 ± 2^0C. (Table 2)

Table 2: Organoleptic characterization of Standard Rabeprazole sodium

Parameters	Reference value	Experimental value
Physical state	Solid	Solid
Colour	White or off-white	Off-white
Melting point	140 ± 1^0C	140 ± 2^0C

Solubility of Rabeprazole sodium

Solubility of Rabeprazole sodium was determined in distilled water, methanol, ethanol, chloroform, ethyl acetate, ether and hexane. (Table 3)

Table 3: Solubility study of standard Rabeprazole sodium

Solvent	Inference
Distilled Water	Very soluble
Methanol	Very soluble
Ethanol	Freely soluble
Chloroform	Soluble
Ethyl Acetate	Soluble
Ether	Insoluble
n-Hexane	Insoluble

FT-IR spectral analysis of pure Rabeprazole sodium

A FT-IR spectrum of pure Rabeprazole sodium was recorded by FT-IR spectroscopy (Shimadzu-8400 S, Japan). FT-IR spectra of Rabeprazole sodium was shown in Fig.

The IR spectrum of pure drug Rabeprazole sodium showed the characteristic peaks at 3134.04 cm-1 for C-H stretching (aromatic) band, 3016.41 and 2946.10 cm-1 for C-H stretching (aliphatic), 2278.25 cm-1 for -OCH_3 stretching, 1730.03 cm-1 for C=N stretching,1236.98 cm-1 for C-N stretching, 1143.71 cm-1 for S=O stretching and 1049.20 cm-1 for C-O-C stretching as shown in Fig 6.1 and Table 4.

Table 4 :FT-IR analysis of Standard Rabeprazole sodium

Characteristic stretching and bending	Wave numbers (cm^{-1})

International Journal of Pharmaceutical Research and Applications
Volume 7, Issue 3 May-June 2022, pp: 1529-1558 www.ijprajournal.com ISSN: 2456-4494

C-H Stretching (aromatic)	3134.04
C-H Stretching (aliphatic)	3016.41, 2946.10
OCH_3 Stretching	2278.25
C=N Stretching	1730.03
C-N Stretching	1236.98
S=O Stretching	1143.71
C-O-C Stretching	1049.20

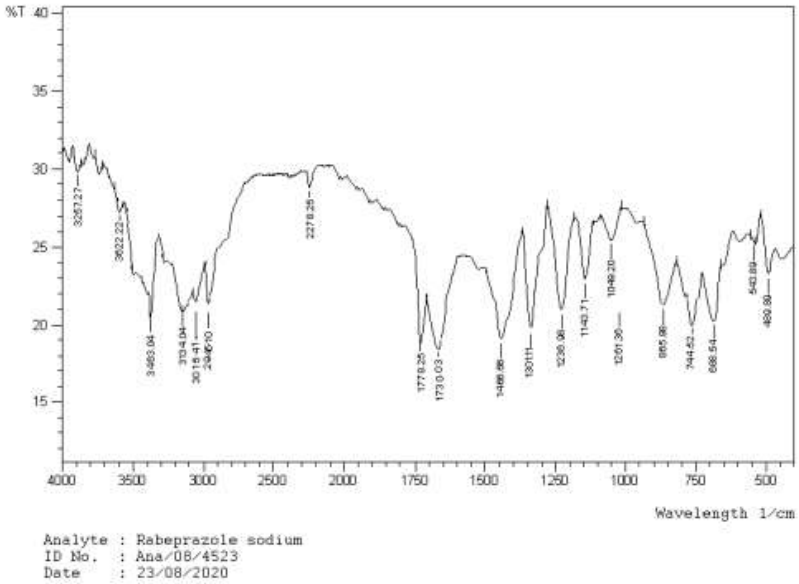

Fig 2: FT-IR spectra of pure Rabeprazole sodium

Determination of $\lambda_{max}$of Rabeprazole sodium

The λ_{max} was measured by UV-VIS double beam spectrophotometer (Shimadzu-1800, Japan). UV spectrum of Rabeprazole sodium shown in Fig 6.2 which showed that it has λ_{max} of 283.7 nm.

International Journal of Pharmaceutical Research and Applications
Volume 7, Issue 3 May-June 2022, pp: 1529-1558 www.ijprajournal.com ISSN: 2456-4494

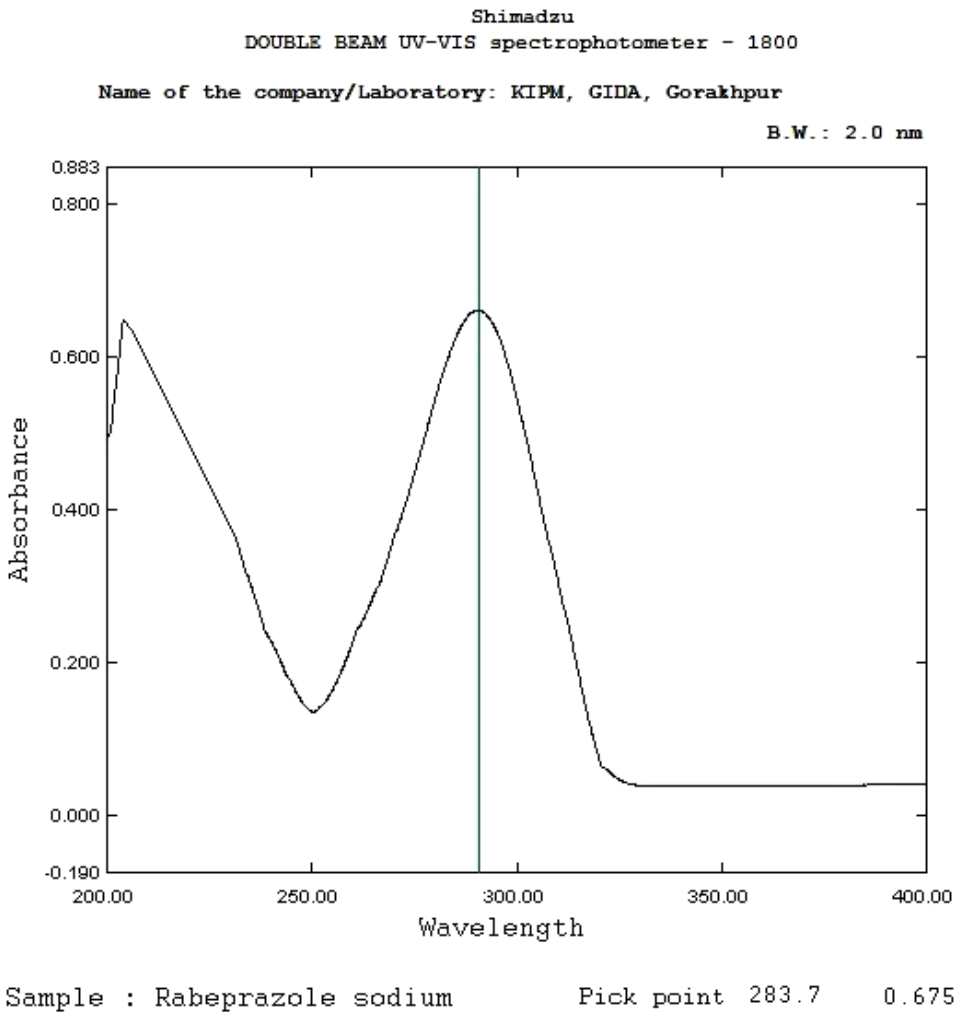

Fig 3: UV spectra of standard Rabeprazole sodium

Standard calibration curve of Rabeprazole sodium

Absorbance obtained for various concentrations of Rabeprazole sodium in 0.1 N HCl are given in Table 6.4. Absorbance data for each dilution was tabulated and graph of concentration versus absorbance was plotted. The graph of absorbance vs. concentration for Rabeprazole sodium was found to be linear Fig 3

Table 5: Absorbance for standard Rabeprazole sodium in 0.1N HCl

Concentration (µg/ml)	**Absorbance at 283.7 nm**
0	0.000 ± 0.064
10	0.231 ± 0.027
20	0.393 ± 0.033
30	0.585 ± 0.021

International Journal of Pharmaceutical Research and Applications
Volume 7, Issue 3 May-June 2022, pp: 1529-1558 www.ijprajournal.com ISSN: 2456-4494

40	0.774 ± 0.063
50	0.937 ± 0.012
All values are expressed as Mean ± SD, (n=3).	

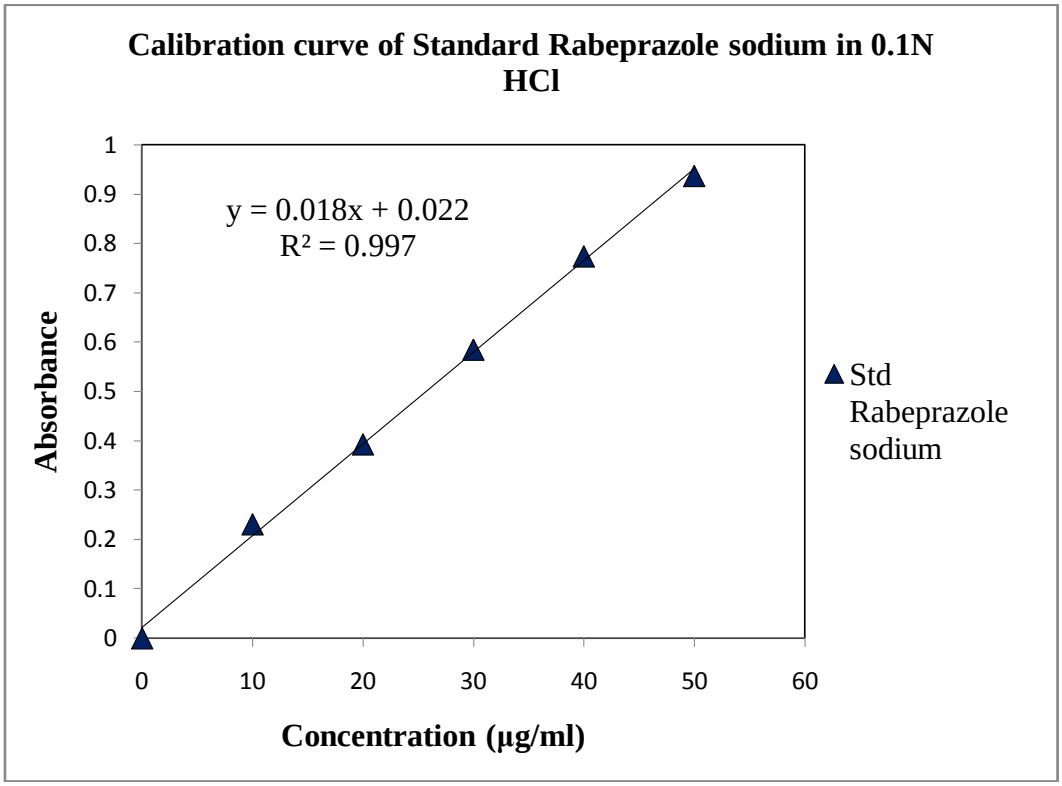

Fig 4: Calibration curve of standard Rabeprazole sodium

Drug-excipients compatibility study

Drug-excipients compatibility study was performed at kept at different temperatures (25 ± 2°C and37 ± 2°C). No change in physical appearance confirms that there was no interaction between drug and polymers used. Concentration of Rabeprazole sodium in different sample withdrawn at different time interval was determined by UV spectrophotometric method. Concentration of Rabeprazole sodium in each sample was determined from the calibration curve of pure drug. The data reveals that percent concentration of Rabeprazole sodium in each sample was significant (Table 6).

IR-spectra of pure drug and with combination of drug + polymers (Ethyl cellulose+HPMCK15M+Eudragit) were compared. Both spectra showed characteristic peaks of Rabeprazole sodium and there was no major shift in them when combined with polymers. Spectral analysis confirms that there were no interaction between Rabeprazole sodium and polymers used in the formulation of floating microspheres (Fig. 5 and 6). Both stability study and spectral analysis showed that polymers were compatible with Rabeprazole sodium.

Table 6: Rabeprazole sodium-excipients compatibility study

S.	**Drug + % concentration of Rabeprazole sodium**

International Journal of Pharmaceutical Research and Applications
Volume 7, Issue 3 May-June 2022, pp: 1529-1558 www.ijprajournal.com ISSN: 2456-4494

No.	Excipients	Temp.	0th Day	10th Day	15th day	20th Day	30th Day
1	Rabeprazole sodium + Ethyl Cellulose	25 ± 2°C	99.54 ± 0.63	99.22 ± 0.53	99.41 ± 0.04	99.35 ± 0.61	99.52 ± 0.31
		37 ± 2°C	99.01 ± .3499	99.38 ± 0.28	99.32 ± 0.21	99.73 ± 0.15	100.52 ± 0.92
2	Rabeprazole sodium + HPMC K15M	25 ± 2°C	100.01 ± 0.47	99.56 ± 0.22	100.32 ± 0.44	99.74 ± 0.36	100.22 ± 0.63
		37 ± 2°C	99.53 ± 0.49	100.65 ± 0.81	99.89 ± 0.73	99.88 ± 0.52	100.64 ± 0.32
3	Rabeprazole sodium + Eudragit	25 ± 2°C	99.76 ± 0.52	99.83 ± 0.64	99.55 ± 0.52	100.34 ± 0.53	99.54 ± 0.35
		37 ± 2°C	99.75 ± 0.65	99.69 ± 0.64	99.92 ± 0.33	99.78 ± 0.73	99.58 ± 0.51
4	Rabeprazole sodium + Ethyl Cellulose + HPMC K15M + Eudragit	25 ± 2°C	99.36 ± 0.41	99.85 ± 0.91	99.73 ± 0.28	99.24 ± 0.37	99.44 ± 0.72
		37 ± 2°C	99.83 ± 0.26	99.26 ± 0.27	99.32 ± 0.41	99.62 ± 0.57	99.85 ± 0.41
All values are expressed as Mean ± SD, (n=3).							

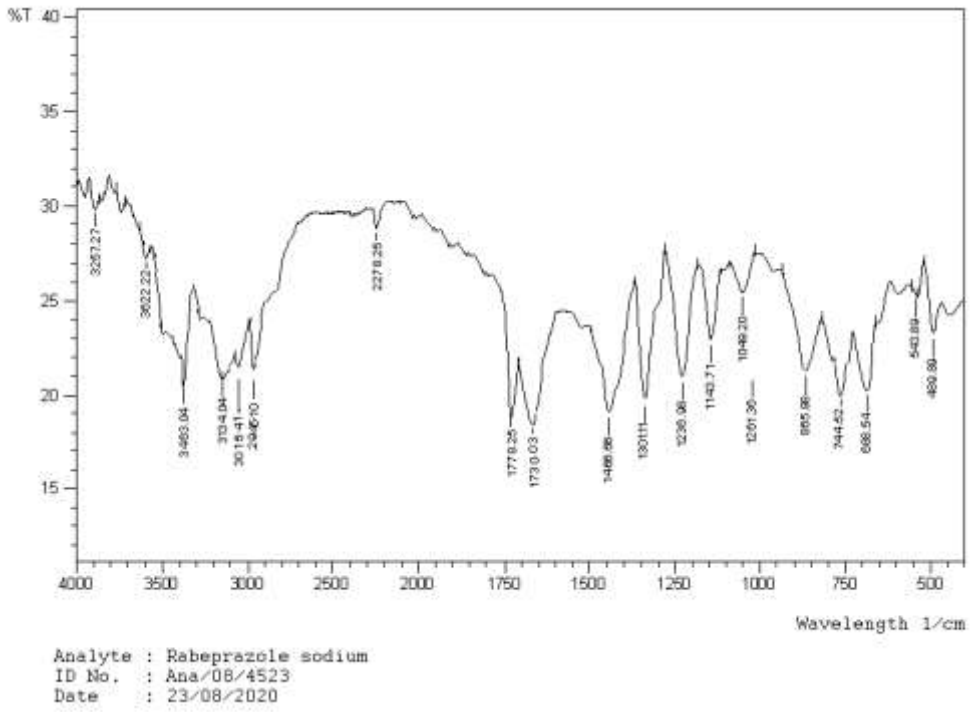

Fig 5: FT-IR spectra of standard Rabeprazole sodium

International Journal of Pharmaceutical Research and Applications
Volume 7, Issue 3 May-June 2022, pp: 1529-1558 www.ijprajournal.com ISSN: 2456-4494

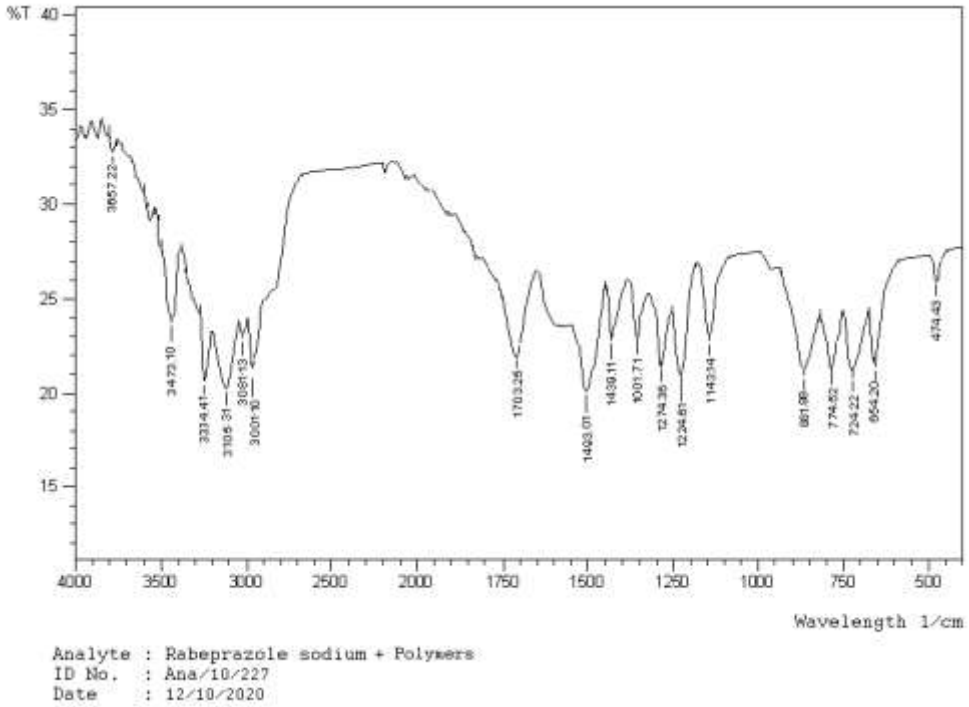

Fig 6: FT-IR spectra of Rabeprazole sodium + polymers

Evaluation of floating microspheres of Rabeprazole sodium

Percentage yield of floating microspheres

All the prepared formulations were dried properly and percentage yield were calculated for each formulation. Highest percentage yield for formulation RZS6 (86.17±0.33) and lowest for formulation RZS2 (80.88±0.67) (Table 7).

Table 7: Percentage yield of floating microspheres

S. No.	Formulations	Theoretical yield (mg)	Practical yield (mg)	Percentage yield (mean ± SD)
1	RZS1	600	489	81.51 ± 0.33
2	RZS2	800	647	80.88 ± 0.67
3	RZS3	1000	824	82.40 ± 0.28
4	RZS4	600	517	86.17 ± 0.33
5	RZS5	800	674	84.25 ± 0.67
6	RZS6	1000	867	86.70 ± 0.73
7	RZS7	600	495	82.50 ± 0.72
8	RZS8	800	654	81.75 ± 0.63
9	RZS9	1000	827	82.70 ± 0.67

Determination of bulk density and tapped density

Bulk density and tapped density were calculated for each formulation and tabulated in Table 8.

Table 8: Bulk density and tapped density of floating microspheres

S. No.	Formulations	Bulk density (gm/cm^3)	Tapped density (gm/cm^3)
1	RZS1	0.468 ± 0.031	0.534 ± 0.032
2	RZS2	0.444 ± 0.070	0.512 ± 0.071

International Journal of Pharmaceutical Research and Applications
Volume 7, Issue 3 May-June 2022, pp: 1529-1558 www.ijprajournal.com ISSN: 2456-4494

3	RZS3	0.486 ± 0.110	0.574 ± 0.033
4	RZS4	0.422 ± 0.047	0.491 ± 0.021
5	RZS5	0.406 ± 0.033	0.483 ± 0.072
6	RZS6	0.410 ± 0.211	0.473 ± 0.043
7	RZS7	0.478 ± 0.053	0.543 ± 0.063
8	RZS8	0.474 ± 0.077	0.553 ± 0.023
9	RZS9	0.470 ± 0.053	0.562 ± 0.041

Determination of Carr's compressibility index and Hausner's ratio of floating microspheres

Bulk density and tapped density data were used for the determination of Carr's compressibility index and Hausner's ratio of floating microspheres. The results were summarized in the Table 9.

Table 9: Carr's compressibility index and Hausner's ratioof floating microspheres

S. No.	Formulations	Bulk density (gm/cm^3)	Tapped density (gm/cm^3)	Carr's index	Hausner's ratio
1	RZS1	0.468 ± 0.031	0.534 ± 0.032	12.36 ± 0.217	1.141
2	RZS2	0.444 ± 0.070	0.512 ± 0.071	13.28 ± 0.331	1.153
3	RZS3	0.486 ± 0.110	0.574 ± 0.033	15.33 ± 0.153	1.181
4	RZS4	0.422 ± 0.047	0.491 ± 0.021	14.05 ± 0.513	1.164
5	RZS5	0.406 ± 0.033	0.483 ± 0.072	15.94 ± 0.233	1.190
6	RZS6	0.410 ± 0.211	0.473 ± 0.043	13.32 ± 0.431	1.154
7	RZS7	0.478 ± 0.053	0.543 ± 0.063	11.97 ± 0.721	1.136
8	RZS8	0.474 ± 0.077	0.553 ± 0.023	14.29 ± 0.527	1.167
9	RZS9	0.470 ± 0.053	0.562 ± 0.041	16.37 ± 0.321	1.196

All values are expressed as Mean ± SD, (n=3).

Determination of angle of repose

The angle of repose (θ) of the floating microspheres was determined by a fixed funnel method. The results were summarized in the Table 10. The result showed that as the concentration of polymer increases, the angle of repose increases but the data showed that all formulation possessed very good flow property.

Table 10: Angle of repose of floating microspheres

S. No.	Formulations	Angle of repose (θ^0)
1	RZS1	17.12 ± 0.731
2	RZS2	19.37 ± 0.532
3	RZS3	19.78 ± 0.327
4	RZS4	18.34 ± 0.921
5	RZS5	21.43 ± 0.741
6	RZS6	22.72 ± 0.082
7	RZS7	20.71 ± 0.721
8	RZS8	24.23 ± 0.076
9	RZS9	23.41 ± 0.312

International Journal of Pharmaceutical Research and Applications
Volume 7, Issue 3 May-June 2022, pp: 1529-1558 www.ijprajournal.com ISSN: 2456-4494

All values are expressed as Mean ± SD, (n=3).

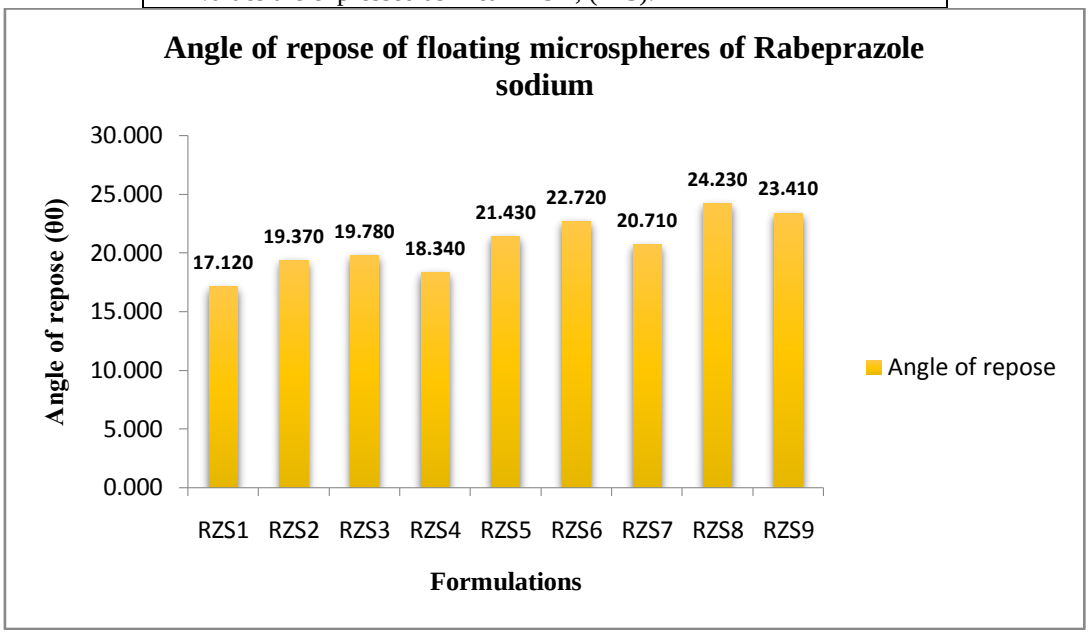

Fig 7: Bar graph of angle of repose of floating microspheres ofRabeprazole sodium

Particle size and particle size distributions analysis

The average diameters of the floating microsphere were determined by an optical microscope method (Table 11 and 12).

Table 11: Average diameters of floating microspheres

S. No.	Formulations	Mean microspheres size (µm)
1	RZS1	85.32 ± 3.213
2	RZS2	87.47 ± 4.373
3	RZS3	86.37 ± 5.361
4	RZS4	111.26 ± 3.761
5	RZS5	117.45 ± 5.231
6	RZS6	121.39 ±7.316
7	RZS7	151.21 ± 5.325
8	RZS8	162.26 ± 3.571
9	RZS9	167.43 ± 4.532

International Journal of Pharmaceutical Research and Applications
Volume 7, Issue 3 May-June 2022, pp: 1529-1558 www.ijprajournal.com ISSN: 2456-4494

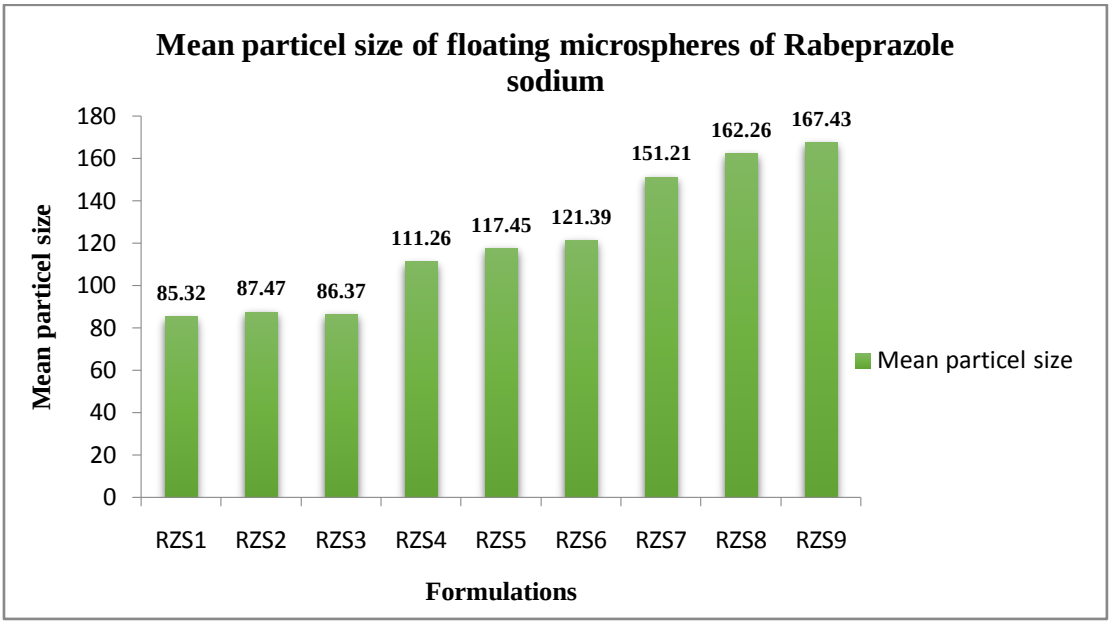

Fig 8: Bar graph of mean particle size of floating microspheres ofRabeprazole sodium

Table 12: Particle size distributions analysis of floating microspheres

Size range (µm)	Formulations								
	RZS1	**RZS2**	**RZS3**	**RZS4**	**RZS5**	**RZS6**	**RZS7**	**RZS8**	**RZS9**
	No. of floating microspheres								
0-50	8	5	4	2	2	1	--	1	1
50-100	62	59	64	48	43	41	32	28	25
100-150	21	31	29	34	37	39	24	22	24
150-200	7	3	2	11	12	15	24	28	30
200-250	2	2	1	4	3	2	12	11	12
250-300	--	--	--	2	3	2	8	10	8

Study of surface morphology (SEM analysis)

Photomicrographs of formulation RZS1, RZS4 and RZS7 (containing equal amount of drug-polymer ratio Fig. 9, 10 and 11) were taken with the help ofscanning electron microscope (JSM 6660D, Tokyo, Japan). SEM photomicrographs of floating microspheres showed that the microspheres were spherical with smooth surface and slightly aggregated.

International Journal of Pharmaceutical Research and Applications
Volume 7, Issue 3 May-June 2022, pp: 1529-1558 www.ijprajournal.com ISSN: 2456-4494

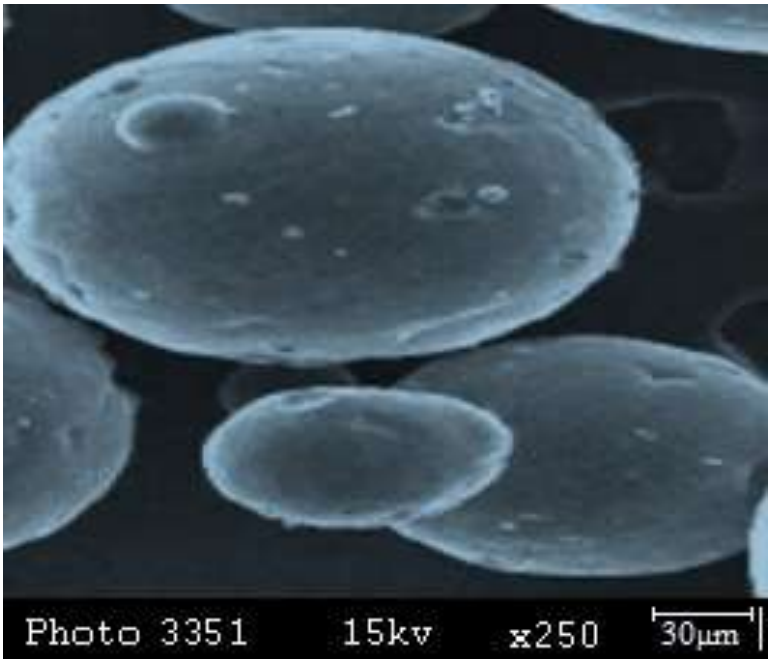

Fig 9: SEM photomicrograph of formulation RZS1

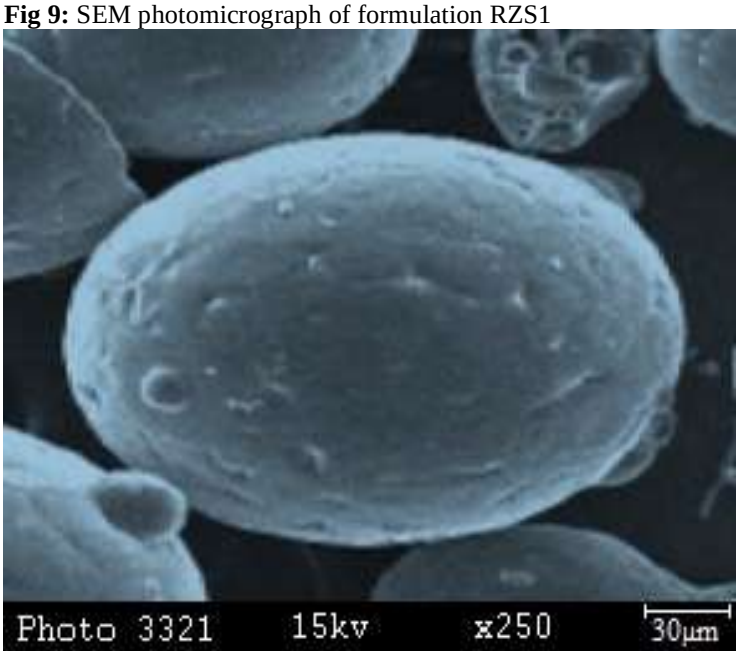

Fig 10: SEM photomicrograph of formulation RZS4

International Journal of Pharmaceutical Research and Applications
Volume 7, Issue 3 May-June 2022, pp: 1529-1558 www.ijprajournal.com ISSN: 2456-4494

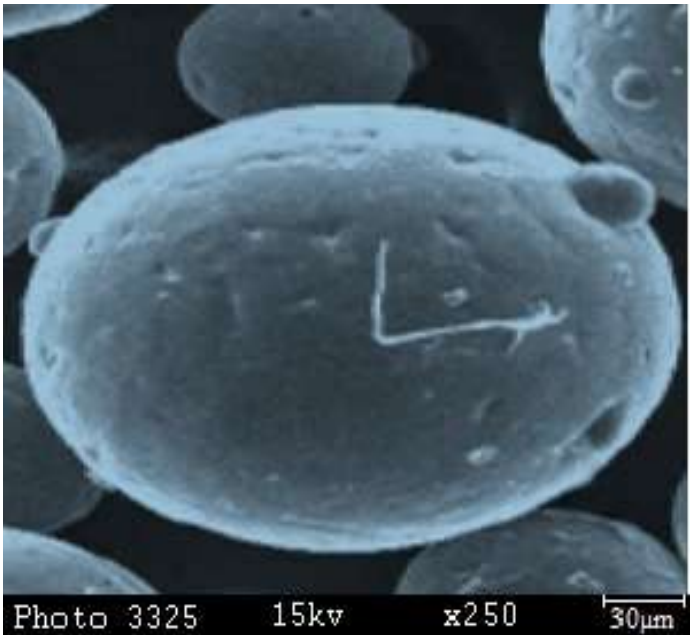

Fig 11: SEM photomicrograph of formulation RZS7

In-vitro percentage buoyancy

Each prepared formulations were evaluated for floating time. Floating ability of microspheres was analyzed as percentage buoyancy. Thepercentage buoyancy of all the formulations was found to be in the range of 62.21 ± 1.337% - 82.70 ± 0.676%. As the concentration of polymers increases, buoyancy also increases. The excellent floating nature of the microspheres may be due to the hollow nature of the microspheres. The result shown that as the particle size increases, floating time of microspheres increases. The results of in-vitro percentage buoyancy are shown in Table 13.

Table 13: Percentage buoyancy of floating microspheres

S. No.	Formulations	Percentage buoyancy of microspheres (%)
1	RZS1	62.21 ± 1.337
2	RZS2	63.85 ± 0.671
3	RZS3	65.03 ±1.286
4	RZS4	67.27 ± 0.233
5	RZS5	69.25 ± 1.112
6	RZS6	73.70 ± 1.323
7	RZS7	71.50 0.725
8	RZS8	76.75 ± 1.633
9	RZS9	82.70 ± 0.676
All values are expressed as Mean ± SD, (n=3).		

International Journal of Pharmaceutical Research and Applications
Volume 7, Issue 3 May-June 2022, pp: 1529-1558 www.ijprajournal.com ISSN: 2456-4494

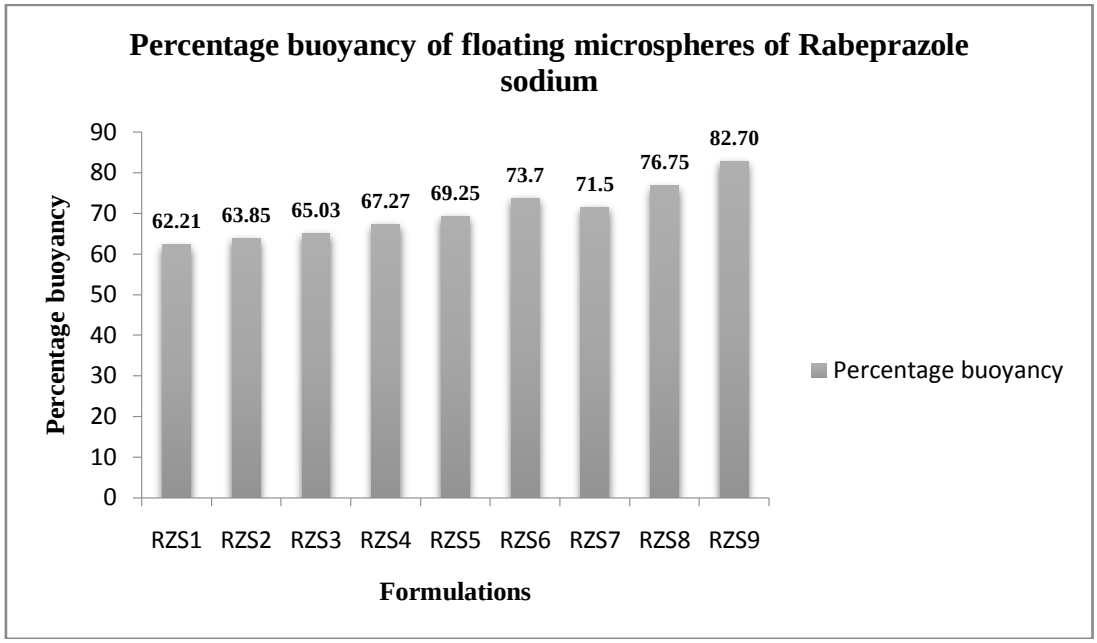

Fig 12: Bar graph of percentage buoyancy of floating microspheres ofRabeprazole sodium

Determination of percentage drug entrapment

Drug entrapment efficiency of each formulation were calculated and shown in Table 14. The data showed that as the concentration of polymer increases, the percentage drug entrapment capability increases. This is due to the high drug encapsulation with the polymers which leads less migration of drug into aqueous phase. The percentage entrapment efficiency for the formulations (RZS1, RZS2 and RZS3) was found to be 69.89 ± 1.832% to 77.68 ± 1.173%. The percentage entrapment efficiency for the formulations (RZS4, RZS5 and RZS6) was found to be 66.93 ± 0.821% to 70.69 ± 1.363%. The percentage entrapment efficiency for the formulations (RZS7, RZS8 and RZS9) was found to be 66.93 ± 1.641% to 73.65 ± 0.721%.

Table 14: Drug entrapment efficiency of floating microspheres

Formulations	Absorbance	Practical drug content in microspheres (µg/ml)	Theoretical drug content in microspheres (µg/ml)	Percentage of drug entrapment
RZS1	0.291	14.46 ± 1.021	20	72.31 ± 1.462
RZS2	0.311	15.53 ± 0.762	20	77.68 ± 1.173
RZS3	0.282	13.97 ± 1.113	20	69.89 ± 1.832
RZS4	0.271	13.38 ± 0.472	20	66.93 ± 0.821
RZS5	0.263	12.95 ± 0.271	20	64.78 ± 1.021
RZS6	0.285	14.13 ± 0.527	20	70.69 ± 1.363
RZS7	0.271	13.38 ± 0.085	20	66.93 ± 1.641
RZS8	0.285	14.13 ± 0.347	20	70.69 ± 1.553
RZS9	0.296	14.73 ± 0.021	20	73.65 ± 0.721
All values are expressed as Mean ± SD, (n=3).				

International Journal of Pharmaceutical Research and Applications
Volume 7, Issue 3 May-June 2022, pp: 1529-1558 www.ijprajournal.com ISSN: 2456-4494

In-vitro drug release study

In-vitro dissolution studies of Rabeprazole sodium from floating microspheres were performed in 0.1N HCl for 12 h using the USP dissolution test apparatus. At specified time intervals, sample aliquots were withdrawn, filtered and diluted with the same. The sample was analyzed spectrophotometrically at 283.7 nm against 0.1N HCl as blank.The results of the in vitro dissolution studies shows controlled and predictable manner as the polymer concentration increases the drug release from the floating microsphere decreases (Table 15, Table 16 and Table 17) (Fig. 13, 14 and 15).

Table 15: Percent cumulative drug release for floating microspheres formulations (RZS1, RZS2 and RZS3)

Time (min)	**RZS1**	**RZS2**	**RZS3**
0	0.00	0.00	0.00
30	12.63	11.33	10.21
60	16.45	14.26	12.23
120	26.43	21.31	18.58
180	36.71	29.48	25.36
240	43.43	36.71	33.71
300	49.37	44.21	40.72
360	57.27	52.74	47.43
420	64.74	59.56	53.67
480	72.52	67.64	61.31
540	78.77	74.33	65.23
600	83.56	79.44	71.56
660	88.45	82.85	75.73
720	93.23	85.32	78.74

International Journal of Pharmaceutical Research and Applications
Volume 7, Issue 3 May-June 2022, pp: 1529-1558 www.ijprajournal.com ISSN: 2456-4494

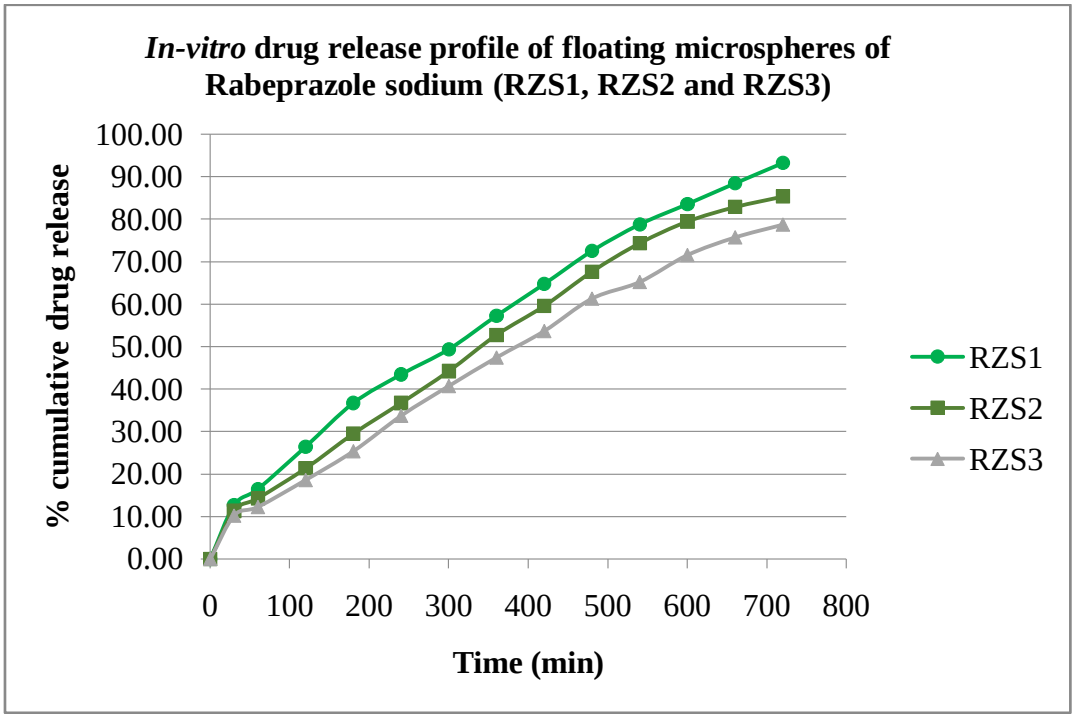

Fig 13: In-vitro drug release profile of floating microspheres ofRabeprazole sodium (RZS1, RZS2 and RZS3)

Table 16: Percent cumulative drug release for floating microspheres formulations (RZS4, RZS5 and RZS6)

Time (min)	**RZS4**	**RZS5**	**RZS6**
0	0.00	0.00	0.00
30	13.54	12.02	11.21
60	18.25	14.53	12.43
120	25.37	19.43	16.35
180	33.54	26.76	22.65
240	38.23	31.11	27.71
300	45.21	38.53	34.13
360	53.76	45.53	39.39
420	61.43	51.37	45.32
480	65.22	57.64	52.52
540	67.17	63.62	56.71
600	71.27	66.71	62.41
660	73.53	69.27	65.33
720	76.42	72.32	68.21

International Journal of Pharmaceutical Research and Applications
Volume 7, Issue 3 May-June 2022, pp: 1529-1558 www.ijprajournal.com ISSN: 2456-4494

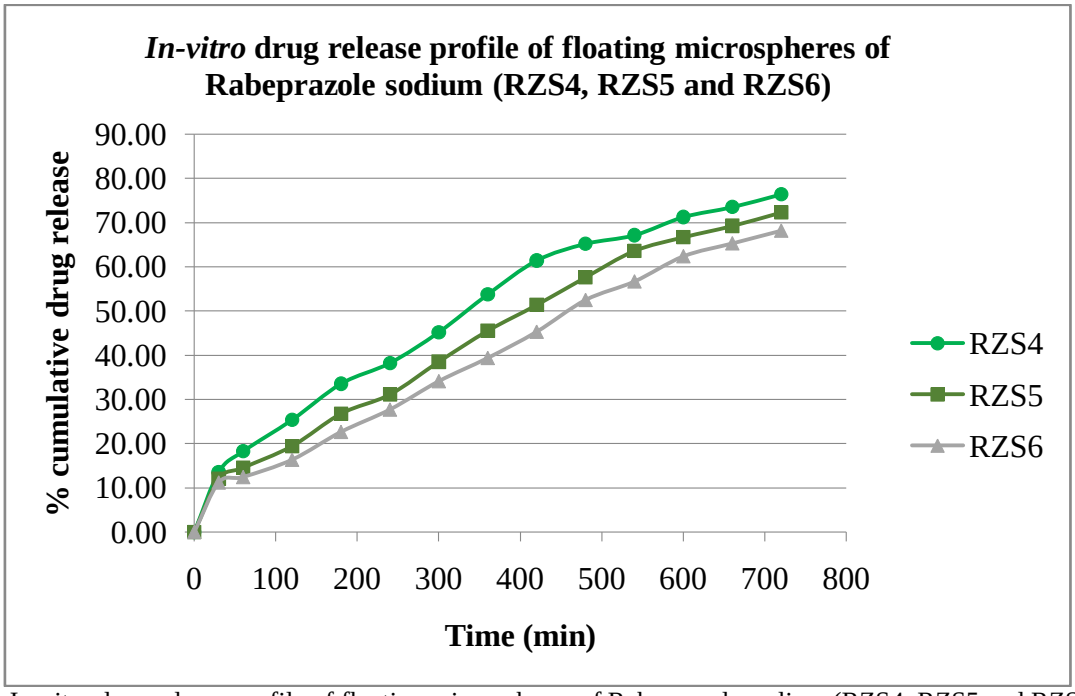

Fig 14: In-vitro drug release profile of floating microspheres of Rabeprazole sodium (RZS4, RZS5 and RZS6)

Table 17: Percent cumulative drug release for floating microspheres formulations (RZS7, RZ8 and RZS9)

Time (min)	RZS7	RZS8	RZS9
0	0.00	0.00	0.00
30	11.23	10.74	9.57
60	15.63	15.01	13.75
120	22.43	21.92	18.43
180	28.72	26.76	23.62
240	33.37	31.73	28.33
300	42.65	36.84	33.52
360	49.54	43.21	37.55
420	54.32	48.63	43.12
480	59.62	54.67	48.82
540	63.24	58.43	52.57
600	65.32	62.34	55.65
660	68.72	64.55	59.62
720	72.32	68.35	62.53

International Journal of Pharmaceutical Research and Applications
Volume 7, Issue 3 May-June 2022, pp: 1529-1558 www.ijprajournal.com ISSN: 2456-4494

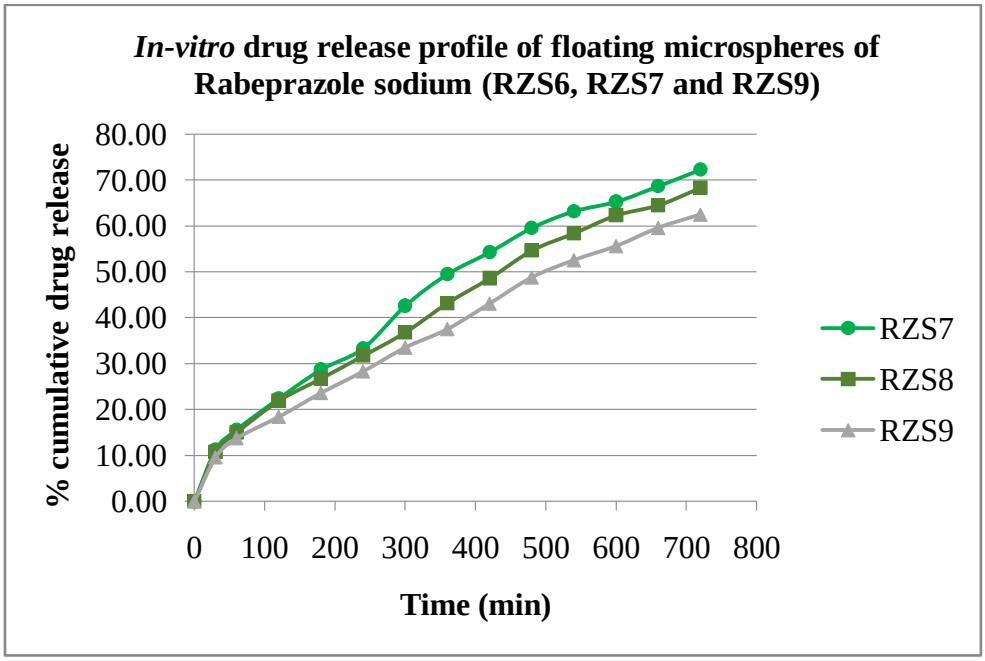

Fig 15: In-vitro drug release profile of floating microspheres of Rabeprazole sodium (RZS7, RZS8 and RZS9)

Drug release kinetic studies

Drug release data were fitted in Zero order rate kinetics, First order rate kinetics and Higuchi's model. Initial drug releases from all formulations were significantly high due to the dissolution of surface adhered drug. As the time increases the release was slow due to the diffusion process.

Zero order release kinetics data

The zero order graphs showed the zero order release characteristics of the formulation, which was confirmed by the correlation value which found to be nearer to one (Table 6.20). Percent cumulative drug release data were represented in Table 18 and graphs shown in Fig. 16, 17 and 18.

Table 18: Percent cumulative drug release from floating microspheres of Rabeprazole sodium formulations.

Time (min)	RZS1	RZS2	RZS3	RZS4	RZS5	RZS6	RZS7	RZS8	RZS9
0	0.00	0.00	0.00	0.00	0.00	0.00	0.00	0.00	0.00
30	12.63	11.33	10.21	13.54	12.02	11.21	11.23	10.74	9.57
60	16.45	14.26	12.23	18.25	14.53	12.43	15.63	15.01	13.75
120	26.43	21.31	18.58	25.37	19.43	16.35	22.43	21.92	18.43
180	36.71	29.48	25.36	33.54	26.76	22.65	28.72	26.76	23.62
240	43.43	36.71	33.71	38.23	31.11	27.71	33.37	31.73	28.33
300	49.37	44.21	40.72	45.21	38.53	34.13	42.65	36.84	33.52
360	57.27	52.74	47.43	53.76	45.53	39.39	49.54	43.21	37.55
420	64.74	59.56	53.67	61.43	51.37	45.32	54.32	48.63	43.12
480	72.52	67.64	61.31	65.22	57.64	52.52	59.62	54.67	48.82
540	78.77	74.33	65.23	67.17	63.62	56.71	63.24	58.43	52.57

International Journal of Pharmaceutical Research and Applications
Volume 7, Issue 3 May-June 2022, pp: 1529-1558 www.ijprajournal.com ISSN: 2456-4494

600	83.56	79.44	71.56	71.27	66.71	62.41	65.32	62.34	55.65
660	88.45	82.85	75.73	73.53	69.27	65.33	68.72	64.55	59.62
720	93.23	85.32	78.74	76.42	72.32	68.21	72.32	68.35	62.53

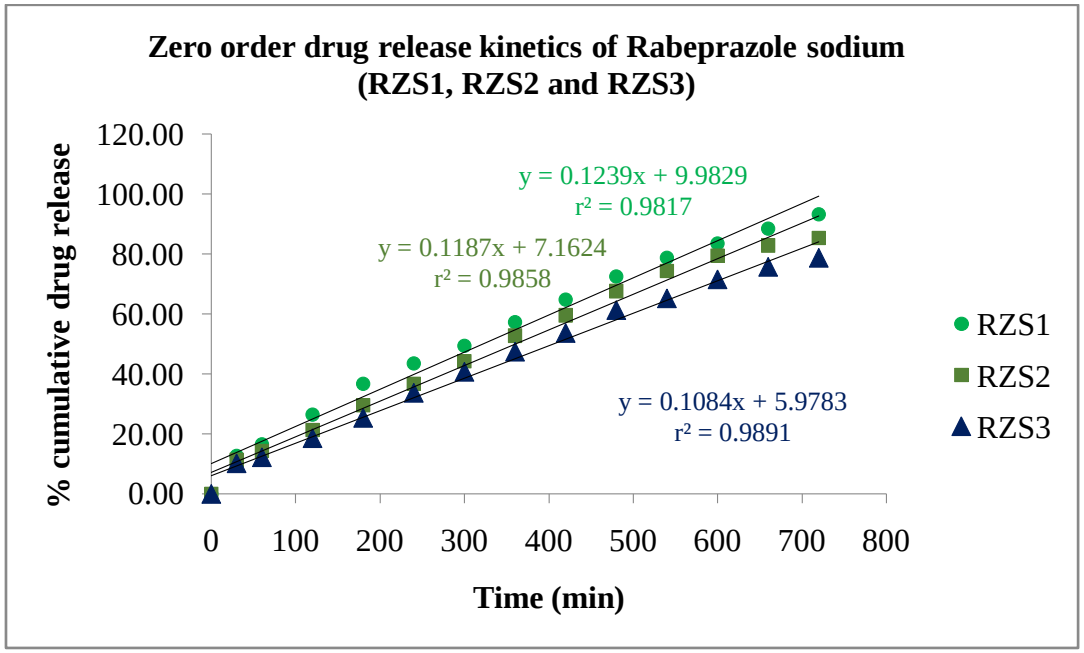

Fig 16: Zero order drug release kinetics of floating microspheres of Rabeprazole sodium formulation (RZS1, RZS2 and RZS3)

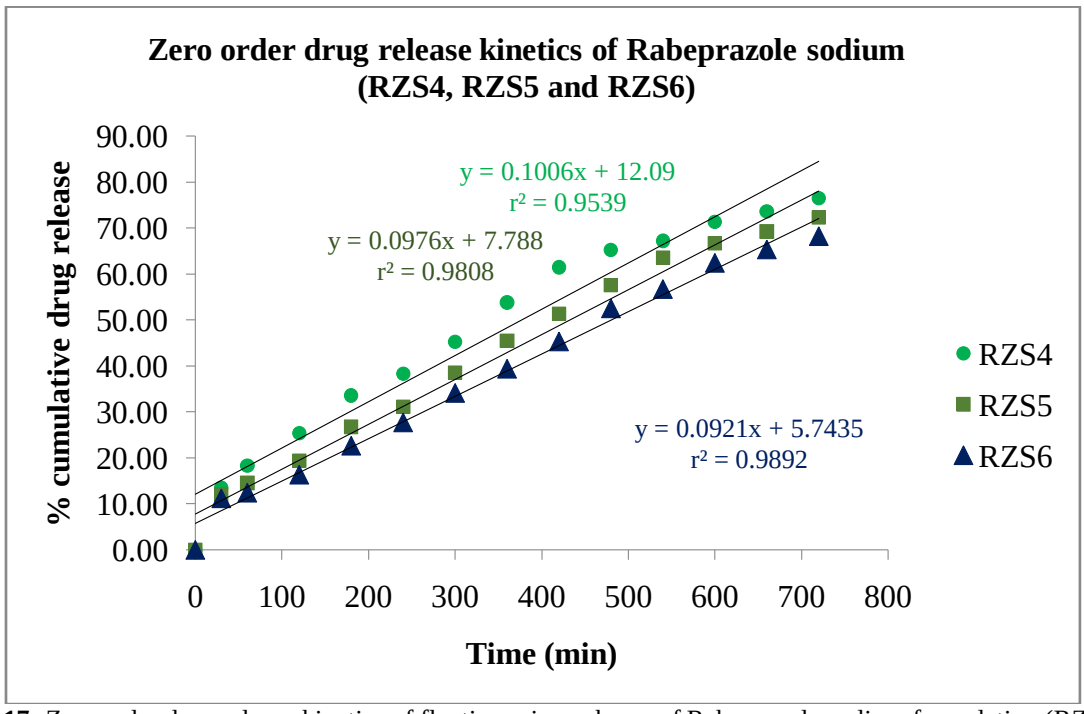

Fig 17: Zero order drug release kinetics of floating microspheres of Rabeprazole sodium formulation (RZS4,

International Journal of Pharmaceutical Research and Applications
Volume 7, Issue 3 May-June 2022, pp: 1529-1558 www.ijprajournal.com ISSN: 2456-4494

RZS5 and RZS6)

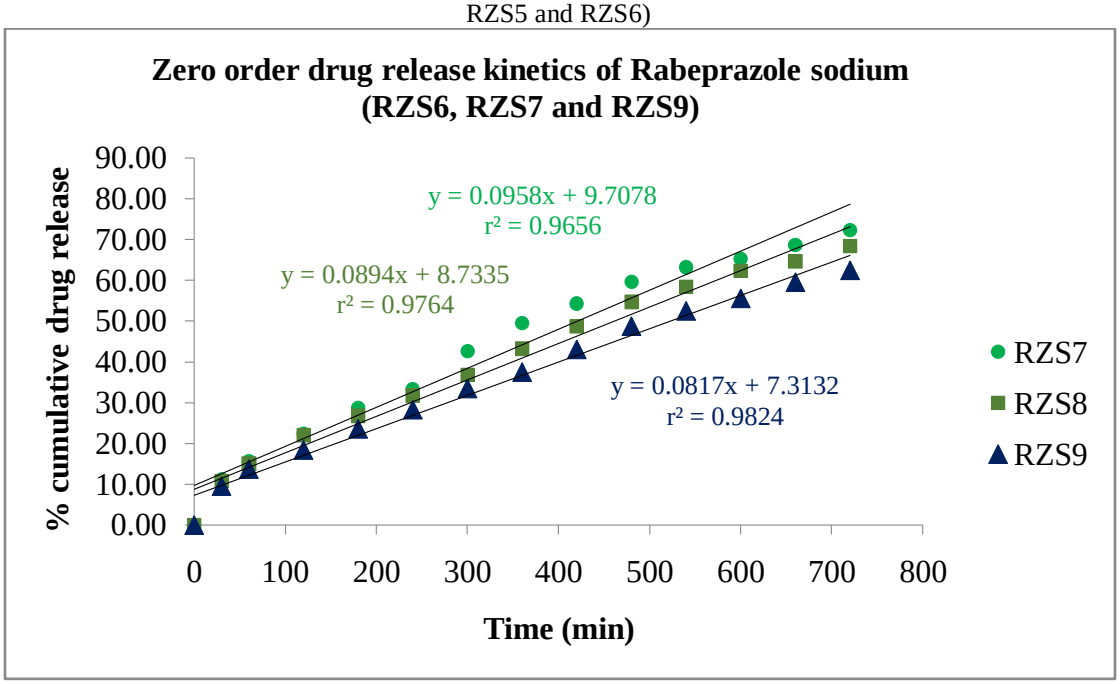

Fig 18: Zero order drug release kinetics of floating microspheres of Rabeprazole sodium formulations (RZS7, RZS8 and RZS9)

First order release kinetics data

The first order graphs showed the first order release characteristics of the formulation, which was confirmed by the correlation value which found to be nearer to one (Table 6.20). Log percent cumulative drug remain to be released from formulations data were represented in Table 19 and graphs shown in Fig. 19, 20 and 21.

Table 19: Log percent cumulative drug remain to be released from floating microspheres of Rabeprazole sodium formulations

Time	RZS1	RZS2	RZS3	RZS4	RZS5	RZS6	RZS7	RZS8	RZS9
0	2.000	2.000	2.000	2.000	2.000	2.000	2.000	2.000	2.000
30	1.941	1.948	1.953	1.937	1.944	1.948	1.948	1.951	1.956
60	1.922	1.933	1.943	1.912	1.932	1.942	1.926	1.929	1.936
120	1.867	1.896	1.911	1.873	1.906	1.922	1.890	1.893	1.912
180	1.801	1.848	1.873	1.823	1.865	1.888	1.853	1.865	1.883
240	1.753	1.801	1.821	1.791	1.838	1.859	1.824	1.834	1.855
300	1.704	1.747	1.773	1.739	1.789	1.819	1.759	1.800	1.823
360	1.631	1.674	1.721	1.665	1.736	1.783	1.703	1.754	1.796
420	1.547	1.607	1.666	1.586	1.687	1.738	1.660	1.711	1.755
480	1.439	1.510	1.588	1.541	1.627	1.677	1.606	1.656	1.709
540	1.327	1.409	1.541	1.516	1.561	1.636	1.565	1.619	1.676
600	1.216	1.313	1.454	1.458	1.522	1.575	1.540	1.576	1.647
660	1.063	1.234	1.385	1.423	1.488	1.540	1.495	1.550	1.606
720	0.831	1.167	1.328	1.373	1.442	1.502	1.442	1.500	1.574

International Journal of Pharmaceutical Research and Applications
Volume 7, Issue 3 May-June 2022, pp: 1529-1558 www.ijprajournal.com ISSN: 2456-4494

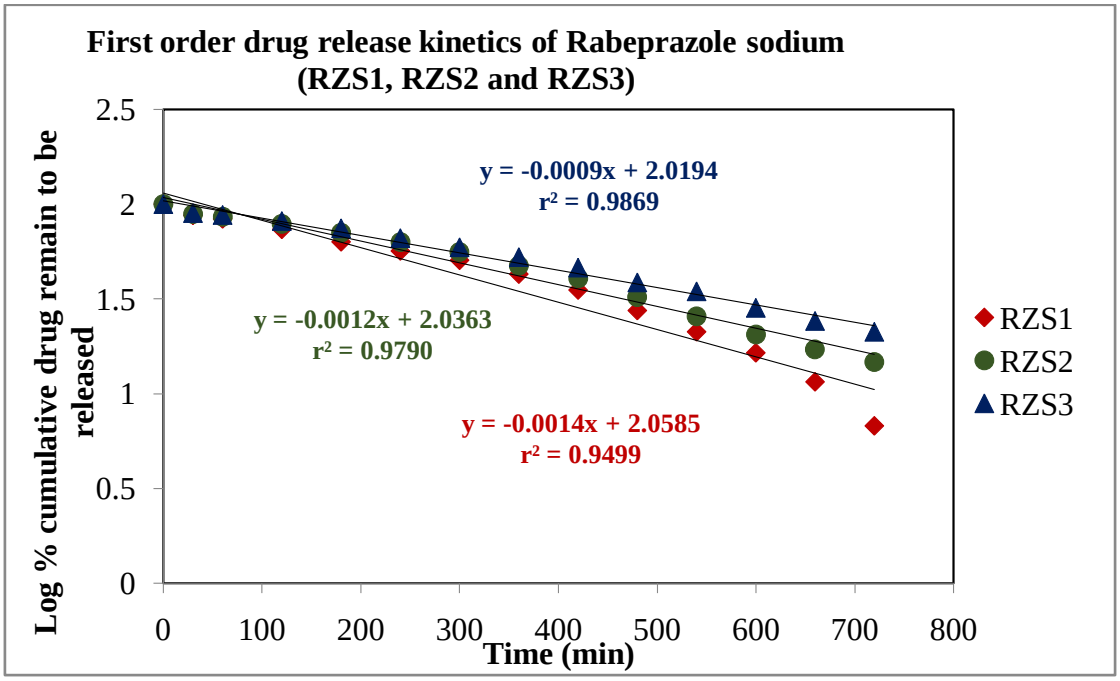

Fig 19: First order drug release kinetics of floating microspheres of Rabeprazole sodium formulation (RZS1, RZS2 and RZS3)

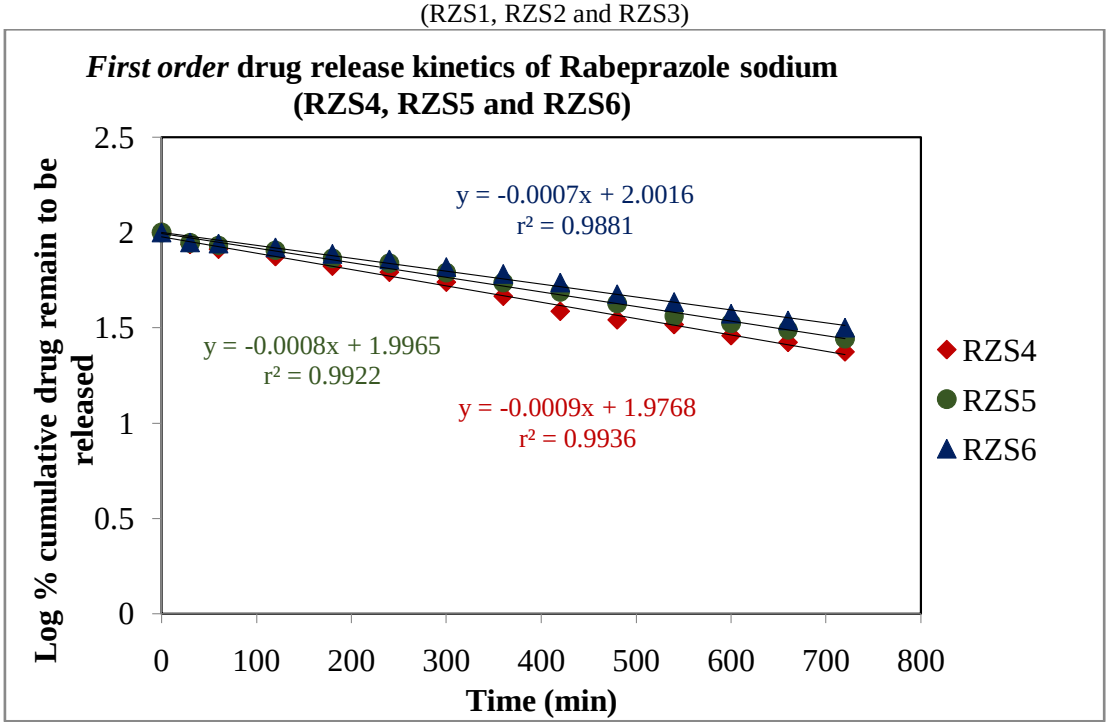

Fig 20: First order drug release kinetics of floating microspheres of Rabeprazole sodium formulation (RZS4, RZS5 and RZS6)

International Journal of Pharmaceutical Research and Applications
Volume 7, Issue 3 May-June 2022, pp: 1529-1558 www.ijprajournal.com ISSN: 2456-4494

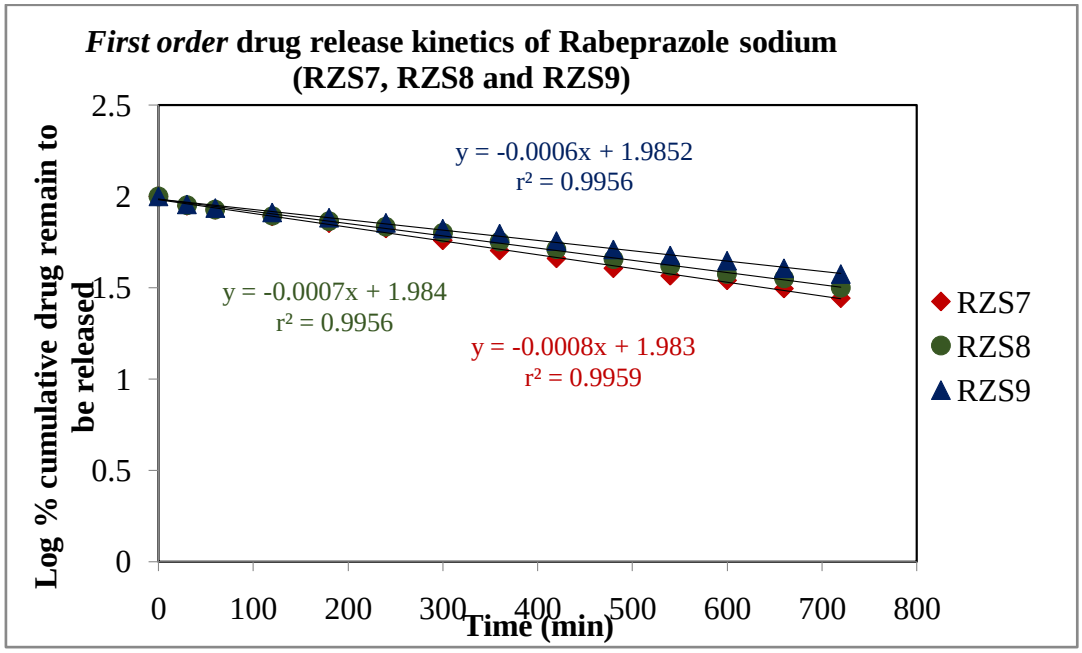

Fig 21: First order drug release kinetics of floating microspheres of Rabeprazole sodium formulation (RZS7, RZS8 and RZS9)

Higuchi's model release kinetics data

Diffusion drug release profile was confirmed by Higuchi's model release kinetics data and correlation value of Higuchi's graph justify that the mechanism of drug release is diffusion (Table 6.20).Percent cumulative drug released from formulations data against square root time were represented in Table 20 and graphs shown in Fig. 22, 23 and 24.

Table 20: Percent cumulative drug release data from floating microspheres of Rabeprazole sodium formulations against $\sqrt{T}$ min (Higuchi's Model)

$\sqrt{T}$ min	RZS1	RZS2	RZS3	RZS4	RZS5	RZS6	RZS7	RZS8	RZS9
0.0000	0.00	0.00	0.00	0.00	0.00	0.00	0.00	0.00	0.00
5.4772	12.63	11.33	10.21	13.54	12.02	11.21	11.23	10.74	9.57
7.7460	16.45	14.26	12.23	18.25	14.53	12.43	15.63	15.01	13.75
10.9545	26.43	21.31	18.58	25.37	19.43	16.35	22.43	21.92	18.43
13.4164	36.71	29.48	25.36	33.54	26.76	22.65	28.72	26.76	23.62
15.4919	43.43	36.71	33.71	38.23	31.11	27.71	33.37	31.73	28.33
17.3205	49.37	44.21	40.72	45.21	38.53	34.13	42.65	36.84	33.52
18.9737	57.27	52.74	47.43	53.76	45.53	39.39	49.54	43.21	37.55
20.4939	64.74	59.56	53.67	61.43	51.37	45.32	54.32	48.63	43.12
21.9089	72.52	67.64	61.31	65.22	57.64	52.52	59.62	54.67	48.82
23.2379	78.77	74.33	65.23	67.17	63.62	56.71	63.24	58.43	52.57
24.4949	83.56	79.44	71.56	71.27	66.71	62.41	65.32	62.34	55.65
25.6905	88.45	82.85	75.73	73.53	69.27	65.33	68.72	64.55	59.62
26.8328	93.23	85.32	78.74	76.42	72.32	68.21	72.32	68.35	62.53

International Journal of Pharmaceutical Research and Applications
Volume 7, Issue 3 May-June 2022, pp: 1529-1558 www.ijprajournal.com ISSN: 2456-4494

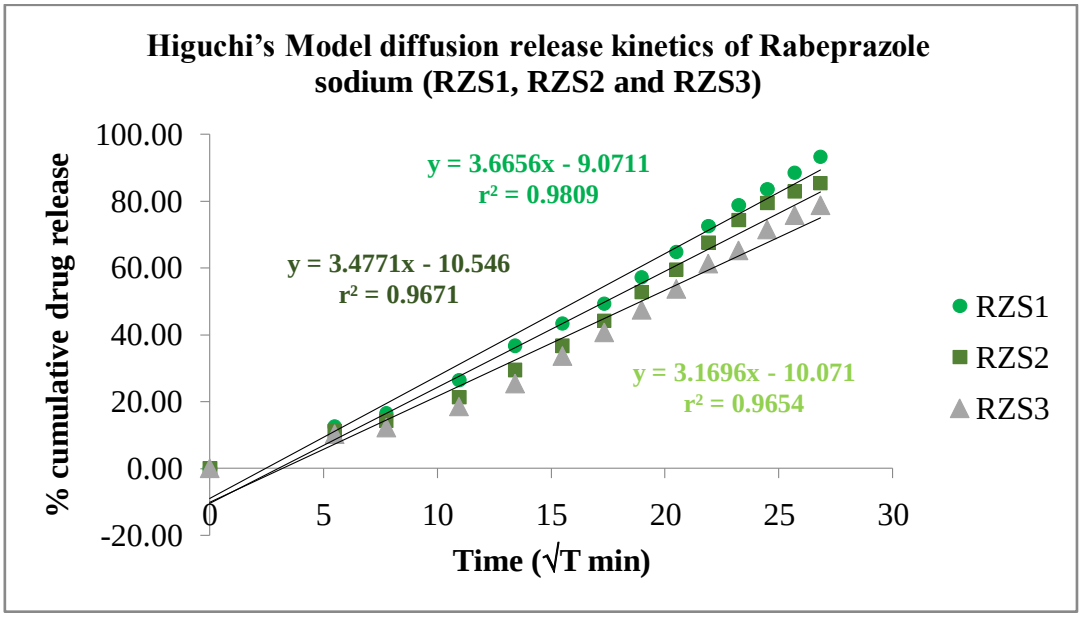

Fig 22: Higuchi's Modeldiffusion release kinetics of floating microspheres of Rabeprazole sodium formulation (RZS1, RZS2 and RZS3)

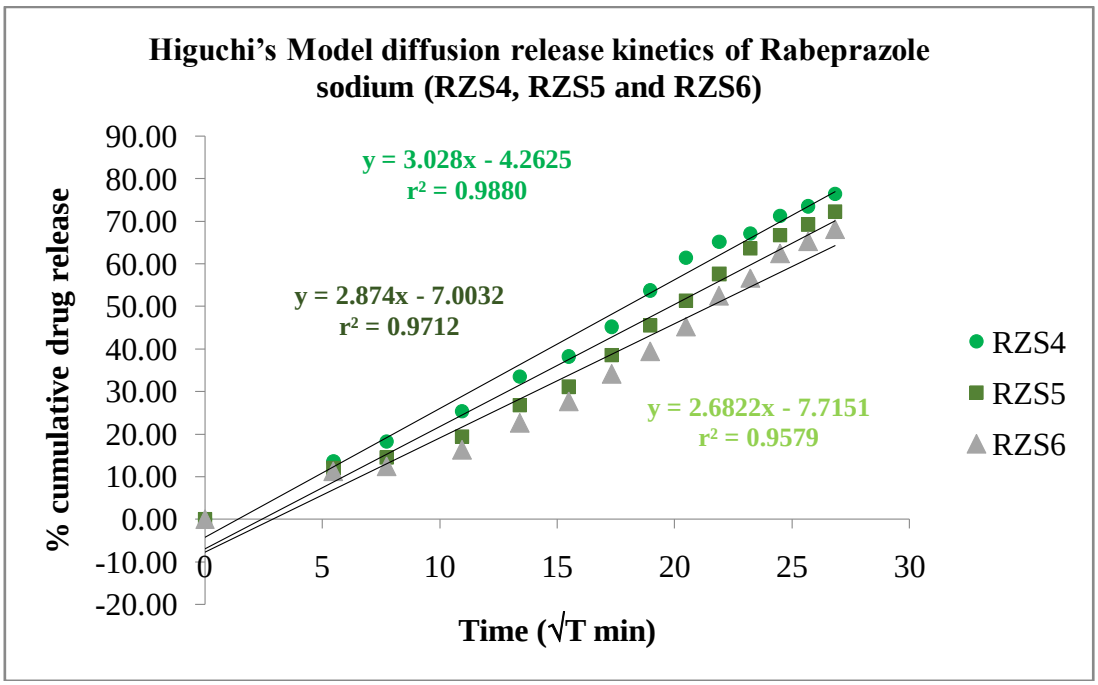

Fig 23: Higuchi's Modeldiffusion release kinetics of floating microspheres of Rabeprazole sodium formulation (RZS4, RZS5 and RZS6)

International Journal of Pharmaceutical Research and Applications
Volume 7, Issue 3 May-June 2022, pp: 1529-1558 www.ijprajournal.com ISSN: 2456-4494

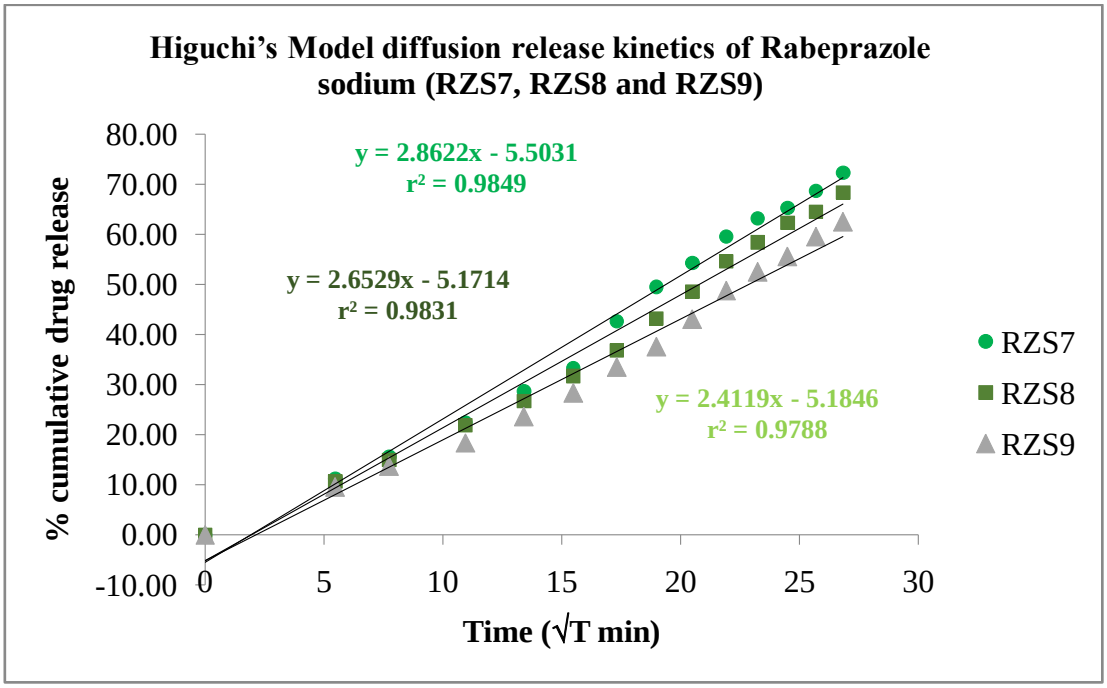

Fig 24: Higuchi's Modeldiffusion release kinetics of floating microspheres of Rabeprazole sodium formulation (RZS7, RZS8 and RZS9)

IV. CONCLUSION

Table 21: Regression co-efficient (r^2) values of different kinetic models

Mechanism of drug release	RZS1	RZS 2	RZS3	RZS4	RZS5	RZS6	RZS7	RZS8	RZS9
	Regression co-efficient (r^2) values								
Zero order drug release kinetics	0.9817	0.9858	0.9891	0.9539	0.9808	0.9892	0.9656	0.9764	0.9824
First order drug release kinetics	0.9499	0.9790	0.9869	0.9936	0.9922	0.9881	0.9959	0.9956	0.9956
Higuchi's Model diffusion release kinetics	0.9809	0.9671	0.9654	0.9880	0.9712	0.9579	0.9849	0.9831	0.9788

International Journal of Pharmaceutical Research and Applications
Volume 7, Issue 3 May-June 2022, pp: 1529-1558 www.ijprajournal.com ISSN: 2456-4494

In total, nine different formulations of Rabeprazole sodium floating microspheres were made using various amounts of polymer. The "Emulsion Solvent Evaporation Technique" was utilised to create Rabeprazole sodium floating microspheres.

Polymer ratios of 1:1, 1:2, and 1:3 (Ethyl cellulose-Eudragit S 100) were used in the formulation. For each of the three formulations, a number was assigned, such as RZS1 through RZS3. Polymer ratios of 1:1, 1:2, and 1:3 were used in the formulation of HPMC K15M-Eudragit S 100. The formulas RZS4, RZS5, and RZS6 were referred to as RZS4. These ratios were employed in the formulation (Ethyl cellulose-HPMC K15M-Eudragit S 100). The three formulations were referred to as RZS7, RZS8, and RZS9 by their respective names.

The normal technique for preformulation studies was followed. A compatibility study was conducted to determine the drug's compatibility with polymers. Rabeprazole sodium is compatible with all polymers used to make floating microspheres, according to FT-IR spectra investigation of Rabeprazole sodium alone and in combination with Ethyl cellulose, HPMC K15M, and Eudragit S 100.

Flow properties, particle size and particle size distributions, surface morphology (SEM analysis), in-vitro percentage buoyancy, drug entrapment, in-vitro drug release, and drug release kinetic analysis were all performed on all nine formulations of Rabeprazole sodium floating microspheres. All nine formulations were found to be effective in achieving the desired drug release concentrations.

It was found that Formulation RZS6 had the highest percentage yield (86.170.33%), whereas Formulation RZS2 had the lowest (80.880.67). As a last check on the formulations' flowability, the bulk density and tapped density were measured on each sample. There was a wide range of particle sizes, from 85.32 3.213 m to 167.434.532 m. According to SEM, microspheres are spherical objects with a smooth surface form.

According to the results, Formulation RZS6 had the highest yield (86,170.33%), while Formulation RZS2 had the lowest (80.880.67). The bulk density and tapped density of each sample were evaluated as a last check on the formulations' flowability.. The particle sizes ranged from 85.32 3.213 m to 167.434.532 m, a broad range. An object with a flat top is known as a microsphere in scanning electron microscopy (SEM).

The results of the in vitro dissolving investigations reveal that when the polymer concentration increases, medication release from the floating microsphere decreases in a controlled and predictable manner.

Drug release data was fit using Higuchi's model, zero order rate kinetics, and first order rate kinetics. Correlation coefficient and Higuchi's graph show that formulations release pharmaceuticals in a zero and first-order manner, respectively.

REFERENCES

[1]. Khar RK, Vyas SP. Targeted and controlled drug delivery novel carrier system, 1st ed.; CBS Publishers and Distributors, New Delhi; 2002; 417-441.
[2]. Jain N K. Advances in Controlled and Novel Drug Delivery, CBS Publisher and Distributors. 2008; 86-90.
[3]. Chien YW. Noval drug delivery system. 2nd ed: Vol. 50, Marcel Dekker Inc., New York; 1992; 161-172.
[4]. Reddy PD, Swarnalatha D. Recent advances in Novel Drug Delivery Systems. International Journal of Pharm Tech Research, 2010; 2(3): 2025-2027.
[5]. Panchagnula R. Transdermal delivery of drugs. Indian J Pharmacol. 1997; 29:140-56.
[6]. Bhagwat RR, Vaidhya IS. Novel Drug Delivery Systems: An Overview, International Journal of Pharmaceutical Sciences and Research, 2013; Vol. 4(3): 970-982.
[7]. Streubel A, Siepmann J, Bodmeier R. Drug delivery to the upper small intestine window using gastroretentive technologies. CurrOpinPharmacol. 2006; 6:501-508.
[8]. Lopes CM, Bettencourt C, Rossi A, Buttini F, Barata P. Overview on gastroretentive drug delivery systems for improving drug bioavailability. Int. J. Pharm. 2016; 510: 144-158.
[9]. Rouge N, Buri P, Doelker E. Drug absorption sites in the gastrointestinal tract and dosage forms for site-specific delivery. Int. J. Pharm. 1996; 136: 117-139.
[10]. Mandal UK, Chatterjee B, Senjoti FG. Gastro-retentive drug delivery systems and their in vivo success: A recent update. Asian J. Pharm. Sci. 2016; 11: 575-584.
[11]. Arora S, Ali J, Ahuja A, Khar RK, Baboota S. Floating drug delivery systems: A review. AAPS Pharm Sci Tech, 2005; 6: E372-E390.

[12]. Garg R, Gupta G. Progress in controlled gastroretentive delivery systems. Trop. J. Pharm. Res. 2008; 7: 1055-1066.
[13]. Garg S, Sharma S. Gastroretentive drug delivery systems. Expert opin. Drug Deliv. 2006; 3: 217-233.
[14]. Clarke G, Newton J, Short M. Gastrointestinal transit of pellets of die ring size and density. Int. J. Pharm. 1993; 100: 81-92.
[15]. Mojaverian P, Vlasses PH, Kellner PE, Rocci ML. Effects of gender, posture, and age on gastric residence time of an indigestible solid: Pharmaceutical considerations. Pharm. Res. 1988; 5: 639-644.
[16]. Krygowska-Wajs A, Cheshire WP, Wszolek ZK, Hubalewska-Dydejczyk A, Jasinska-Myga B, Farrer MJ, Moskala M, Sowa-Staszczak A. Evaluation of gastric emptying in familial and sporadic Parkinson disease. Parkinsonism Relat. D. 2009; 15: 692-696.
[17]. Waugh A, Grant A. Anatomy and physiology in health and illness. 9th ed. Elsevier Churchill Livingstone, Edinburgh; 2001.
[18]. Wilson CG, Washington N. The stomach: its role in oral drug delivery. Physiological Pharmaceutical: Biological Barriers to Drug Absorption. Chichester, UK: Ellis Horwood; 1989; 47-70.
[19]. Fujimori J, Machida Y, Tanaka S, Nagai T. Effect of magnetically controlled gastric residence of sustained release tablets on bioavailability of acetaminophen. Int. J. Pharm. 1995; 119: 47-55.
[20]. Julu T, Prakash T, Ravi M, Seong HJ. Current State and Future Perspectives on Gastroretentive Drug Delivery Systems. Pharmaceutics, 2019; 11:193, 1-22.
[21]. Singh B, Kim KH. Floating drug delivery systems: An approach to oral controlled drug delivery via gastric retention. J Control Rel. 2000; 69: 235-259.
[22]. Mayavanshi AV, Gajjar SS. Floating drug delivery systems to increase gastric retention of drugs: A Review. Research J. Pharm. And Tech. 2008; 1: 345-348.
[23]. Dolas RT, Hosmani A, Bhandari A, Kumar B, Somvanshi S. Novel Sustained Release Gastroretentive Drug Delivery System: A Review. International Journal of Pharma Research and Development 2011; 2(1): 26-41.
[24]. Chretien C, Boudy V, Allain P, Chaumei JC. Indomethacin release from ion-exchange microspheres: impregnation with alginate reduces release rate. Journal of Controlled Release 2004; 96: 369-378.
[25]. Mathur P, Verma N. Floating drug delivery system: An innovative acceptable approach in gastroretentive drug delivery. Scholars Research Library 2010; 2(2): 257-70.
[26]. Rahim SA, Carter P, Elkordy AA. Influence of calcium carbonate and sodium carbonate gassing agents on pentoxifylline floating tablets properties. Powder Technol. 2017; 322: 65-74.
[27]. Baumgartner S, Kristl J, Vrecer F, Vodopivec P, Zorko B. Optimisation of floating matrix tablets and evaluation of their gastric residence time. Int. J. Pharm. 2000; 195: 125-135.
[28]. Chandel A, Chauhan K, Parashar B, Kumar H, Arora S. Floating drug delivery systems: A better approach. International Current Pharmaceutical Journal 2012; 1(5): 110-118.
[29]. Shah SH, Patel JK, Patel NV. Stomach specific floating drug delivery system: A review. International Journal of Pharmaceutical Technology and Research 2009; 1(3): 623-633.
[30]. Møller MH, Adamsen S, Wøjdemann M, Møller AM. Perforated peptic ulcer: how to improve outcome?.Scand J Gastroenterol, 2009; 44: 15-22.
[31]. Manfredini R, Giorgio RD, Smolensky MH, Boari B, Fabbri D, Contato E, Serra M, Barbara G, Stanghellini V, Corinaldesi R, Gallerani M. Seasonal pattern of peptic ulcer hospitalizations: analysis of the hospital discharge data of the Emilia-Romagna region of Italy. BMC Gastroenterol, 2010; 10: 37.
[32]. Janik J, Chwirot P. Perforated peptic ulcer–time trends and patterns over 20 years. Med Sci Monit, 2000; 6: 369-372.
[33]. Watts DD, Fakhry SM. Incidence of hollow viscous injury in blunt trauma: an analysis from 275,557 trauma admissions from the East multi-institutional trial. J Trauma 2003; 54: 289-294.
[34]. Oosting SF, Peters FT, Hospers GAp, Mulder NH. patient with metastatic melanoma presenting with gastrointestinal perforation after dacarbazine infusion: a case report. J Med Case Reports 2010; 4: 10.
[35]. Golffier C, Holguin F, Kobayashi A. A Duodenal perforation because of swallowed

ballpoint pen and its laparoscopic management:report of a case. J Pediatr Surg. 2009; 44: 634-636.
[36]. Bianchini AU, Mehta SN, Mulder DS, Barkun AN, Mayrand S. Duodenal perforation by a Greenfield filter: endoscopic diagnosis. Am J Gastroenterol, 1997; 92: 686-687.
[37]. So JB, Yam A, Cheah WK, Kum CK, Goh PM. Risk factors related to operative mortality and morbidity in patients undergoing emergency gastrectomy. Br J Surg, 2000; 87: 1702-1707.
[38]. Rozycki GS, Ballard RB, Feliciano DV, SchmidtJA, Pennington SD. Surgeon-performed ultrasound for the assessment of truncal injuries. Ann Surg, 1998; 228: 557.
[39]. Tripathi KD. Essential of medical pharmacology. Drug for peptic ulcer, 6th edition, Jaypee publication, 2008; 627-640.
[40]. Pachuau L, Sarkar S, Mazumder B. Formulation and evaluation of matrix microspheres for simultaneous delivery of salbutamol sulphate and theophylline. Trop J Pharm Res 2008; 7(2): 995-1002.
[41]. Ramesh PC, Harshad GP, Hiren JP, Dushyant A. Microparticulate system: a revolution in drug delivery. IJPI's Journal of Pharmaceutics and Cosmetology, 2010, 1:1.
[42]. Deshpande AA, Rhodes CT, Shah NH, Malick AW, Controlled-release drug delivery systems for prolonged gastric residence: an overview, Drug Dev. Ind. Pharm 1996; 531-539.
[43]. Gunja c, Prakash B, SahaR.N.Microspheres technology and its applications. (PDF). http://docstoc.com/docs/38166355/review-on-microspheres, Nov 2010.
[44]. Alagusundaram M, Madhu SC, Umashankari K, Venkata BA, Lavanya C, Ramkanth S. Microspheres As A Novel Drug Delivery Sysytem - A Review. Int J Chem Tech Res. 2009; 1(3): 526- 534.
[45]. Vikrant KN, Gudsoorkar VR, Hiremath SN, Dolas RT, Kashid VA. Microspheres-A Novel Drug Delivery: An Overview. Int J Pharmaceutical and Chem Sciences. 2012; 1(1): 113-128.
[46]. Choi BY, Park HJ, Hwang SJ. Preparation of alginate beads for floating drug delivery system effects of CO_2 gas forming agents. Int. J. Pharm. 2002; 239: 81-91.
[47]. Indian Pharmacopoeia. Vol. 1. The Indian Pharmacopoeia Commission, Ghaziabad, 2007, 107.
[48]. Talukder R, Fassihi R. Gastro retentive delivery systems: a mini review, Drug Dev. Ind. Pharm, 2002; 30; 1019-1028.
[49]. Ogawa Y, Yamamoto M, Hokada, Yashiki T, Shimamoto T. Chem. Pharm. A new technique to efficiently entrap leuprolide acetate into microcapsules of polylactic acid or copoly (lactic/glycolic) acid Bull. 1998; 36: 1095-1103.
[50]. EMathiowitz RJ. Polyanhydride microspheres as drug carriers I. Hot-melt microencapsulation. Journal of controlled Release, 1987; 5: 13-22.